Applied Energy 391 (2025) 125858

Contents lists available at ScienceDirect

Applied Energy

journal homepage: www.elsevier.com/locate/apenergy

Techno-economic performance of reservoir thermal energy storage for data center cooling system

Hyunjun Oh [a,*], Wencheng Jin [b,c], Peng Peng [d,e], Jeffrey A. Winick [f], David Sickinger [a], Dale Sartor [d], Yingqi Zhang [d], Koenraad Beckers [a], Kevin Kitz [g], Diana Acero-Allard [a], Trevor A. Atkinson [b], Patrick Dobson [d]

[a] National Renewable Energy Laboratory, Golden, CO, USA
[b] Idaho National Laboratory, Idaho Falls, ID, USA
[c] Texas A&M University, College Station, TX, USA
[d] Lawrence Berkeley National Laboratory, Berkeley, California, USA
[e] State Key Laboratory of Mesoscience and Engineering, Institute of Process Engineering, Chinese Academy of Sciences, Beijing, China
[f] U.S. Department of Energy, Golden, CO, USA
[g] KitzWorks LLC, Boise, ID, USA

HIGHLIGHTS

- The RTES reliably supplies a 5 MW data center cooling load over the 20-year lifetime.
- The coefficient of performance of the RTES is 16.5 during the summer peak.
- The levelized cost of cooling of the RTES system is $5/MWh.
- The RTES significantly saves electricity consumption and costs (78 % and 83 %, respectively), compared to the base case.
- 78 % of annual CO_2 emissions are avoided with the RTES compared to the base case.

GRAPHICAL ABSTRACT

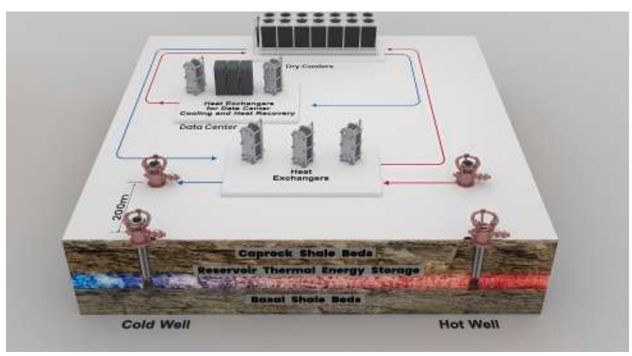

ARTICLE INFO

Keywords:
Data center cooling
Reservoir thermal energy storage
RTES
Techno-economic analysis
Levelized cost of cooling
LCOC

ABSTRACT

Electronic equipment in data centers generates heat during operation, which should be dissipated through a cooling system to prevent overheating and maintain optimal performance. Electricity consumption for the data center cooling system becomes significant as the demand for data-intensive services increases. Although various technologies have been developed and integrated into the data center cooling system, there are limited high-efficiency alternatives for data center cooling. In this study, we designed a reservoir thermal energy storage (RTES) system that stores cooling energy during winters and produces it during summers for data center cooling. We then demonstrated the techno-economic performance of the RTES incorporated with dry coolers and heat recovery for a year-round 5 MW cooling load. The RTES cooling production was reliable during the 20-year lifetime. We estimated the levelized cost of cooling as $5/MWh, significantly lower than $15/MWh for the base scenario where chillers and dry coolers supply the same cooling load without the RTES. We also estimated

* Corresponding author.
E-mail address: hyunjun.oh@nrel.gov (H. Oh).

https://doi.org/10.1016/j.apenergy.2025.125858
Received 9 November 2024; Received in revised form 9 March 2025; Accepted 3 April 2025
Available online 11 April 2025

that the RTES-based cooling system annually avoids CO_2 emissions up to 1488 tCO_2e compared to the base case. These results highlight techno-economic feasibility and environmental benefits of the RTES and its potential to be deployed for various applications at large scales as well as for data center cooling.

1. Introduction

The demand for data center services increases rapidly with an increase in data-intensive workloads, such as artificial intelligence [1–5]. Global data center electricity consumption grew from 194 TWh in 2010 to 205 TWh in 2018, representing about 1 % of the world's electricity consumption in 2018, even though advances in computing efficiency helped offset the growth in total energy use by the information and communication technology (ICT) equipment [6]. More recently, the International Energy Agency (IEA) estimated that electricity consumption from data centers, artificial intelligence, and the cryptocurrency sector reached 460 TWh in 2022 and could exceed 1000 TWh in 2026 [7]. A data center can be more than 40 times as energy intensive as conventional office buildings [8], and large-scale data centers are often considered to be industrial facilities, rather than commercial buildings, in terms of electricity consumption [9].

In the United States, data center energy demand is concentrated in specific regions, such as Northern Virginia and California [10,11]. The U.S. data center sector consumed 61 TWh in 2006, representing roughly 1.5 % of total U.S. electricity consumption [9] and increased to 70 TWh in 2014, representing about 1.8 % of total U.S. electricity consumption [12]. Although the increase in the U.S. data center sector's electricity consumption was relatively stable between 2014 and 2016, it began to rise significantly in 2017, driven by the expansion of the base of installed servers and the growing prevalence of accelerated servers for graphics processing units to support artificial intelligence [5]. By 2018, data center electricity consumption had reached approximately 76 TWh, representing 1.9 % of total annual U.S. electricity consumption. Since then, U.S. data center electricity consumption has rapidly grown, reaching 176 TWh in 2023 (4.4 % of total U.S. consumption), and is projected to range between 325 and 580 TWh by 2028, accounting for 6.7 % to 12.0 % of total U.S. electricity consumption [5]. Similarly, Electric Power Research Institute (EPRI) reported that the electricity consumption in the U.S. data centers increased at an increasingly rapid pace approximately from 75 TWh in 2020 to 152 TWh in 2023 [11].

Data centers consume electricity primarily for operating ICT equipment (the largest share), followed by cooling systems (the second largest) and lighting and ventilation systems (smaller portions) [13]. The energy efficiency of a data center is evaluated using various metrics, including power usage effectiveness (PUE), which is a ratio of total power used in the data center to the power used by ICT equipment, as discussed in studies such as [2,14,15]. For example, if a data center has a PUE of 1.5, 67 % of the total energy consumption is allocated to ICT equipment, and the remaining 33 % is allocated to cooling and other end uses. According to EPRI, the U.S. national average PUE has stabilized at around 1.6, which was the average PUE from 2020 to 2023. A further decrease is projected, with the average PUE potentially approaching 1.2 with advancements in energy-efficient cooling technologies [11]. Similarly, researchers at Lawrence Berkeley National Laboratory estimated the national PUE to be 1.4 in 2023, with projections indicating a further decrease by 2028, from approximately 1.35 to 1.15 [5]. This implies that electricity consumption for cooling accounts for approximately 28 % to 38 % of total energy consumption in the U.S. data center sector as of 2023. Although the PUE varies by time of day and season depending on environmental and operational conditions [16], the PUE can reach around 1 by advancing and optimizing data center operation [14,15]. A wide range of innovative cooling solutions have been developed and implemented to reliably and efficiently operate ICT equipment and achieve a low PUE.

In addition to ensuring energy-efficient data center operations (i.e., achieving a lower PUE), hardware components in ICT equipment (e.g., processor, RAM) generate heat during operation, which should be dissipated to minimize potential damage from overheating. To maintain a safe operating temperature, cold water and/or air are circulated through the ICT equipment and server racks in cabinets, and the thermal energy gained is rejected using various heat rejection alternatives. Examples of cooling systems include cold plates, immersion liquid cooling, computer room air conditioning/handling (CRAC/CRAH) units, two-phase heat pipe/thermosiphon systems, dry coolers, and thermal energy storage systems [17]. In addition to the heat rejection through cooling systems, thermal energy produced from the ICT equipment operations can be utilized as useful energy for various heat recovery applications including direct-use or heat pump-based heating systems [18,19].

Recently, geological thermal energy storage systems have attracted attention as sustainable and reliable energy systems. Aquifer thermal energy storage (ATES), which utilizes an aquifer layer to store and produce thermal energy, has been developed and deployed over decades. Fleuchaus et al. [20] reported in 2018 that more than 2800 ATES systems are in operation worldwide. More recently, the ATES concept was extended to a low-quality groundwater layer in deeper permeable formations (e.g., brackish reservoir); this new system is defined as reservoir thermal energy storage (RTES) [21]. Even though the capital cost for drilling deeper wells in the RTES system is higher than the ATES well drilling cost [22], the RTES typically provides a better environment by utilizing slow-moving, geochemically evolved, and thermally insulated aquifers in deeper geologic formations to store thermal energy [21,23]. The RTES operation in deeper formations also minimally affects fresh groundwater systems in a shallow subsurface. Although the low-quality groundwater resources in deep formations have those advantages and great potential as an energy system (similar to hydrothermal resources for a geothermal energy system), there are only limited studies on RTES systems (e.g., [24,25]), particularly for cold energy storage [26].

In this study, we designed two RTES-based cooling systems incorporated with dry coolers (Scenario 2) and dry coolers and heat recovery (Scenario 3) for supplying 5 MW cooling load from a data center in Golden, Colorado, USA. We modeled the 20-year RTES system operations to reliably meet the data center cooling load while ensuring that cooling production and recharging were balanced throughout the system's lifetime. In Scenario 3, we assumed 50 % of thermal energy produced in the data center was recovered during winter for the building's water heating load and, correspondingly, the RTES and dry cooler operations were reduced. The techno-economic performance of the two RTES-based data center cooling systems was then evaluated by comparing electricity consumption, capital and operational costs, and levelized cost of cooling (LCOC) to those of the base case (Scenario 1) where the same load was supplied by chillers and dry coolers. Because techno-economic analysis, particularly the LCOC, of data center cooling systems and RTES systems has been limited in the literature, the results of this study will provide valuable insights into the feasibility and cost-effectiveness of both non-RTES and RTES-based data center cooling solutions.

2. Methods

2.1. Design of data center cooling system

The cooling technologies considered in this study include the RTES, dry coolers, and chillers, all of which have different advantages and

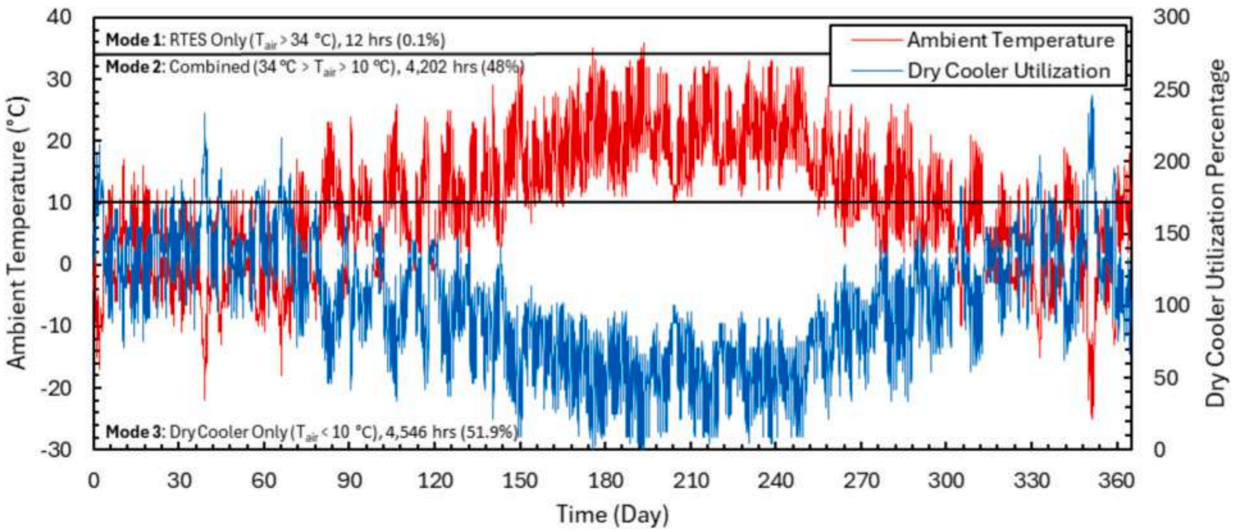

Fig. 1. Three operational modes of dry coolers for data center cooling based on ambient temperature in Golden, Colorado. Dry cooler utilization exceeds 100 % in Mode 3, while the data center cooling load is supplied by the RTES and dry coolers with a capacity reduced below the full capacity in Mode 2.

Table 1
Three operational modes for the data center cooling system in three scenarios.

	Scenario 1	Scenario 2	Scenario 3
Heat Rejection Alternatives	Chillers and dry coolers	RTES and dry coolers	RTES, dry coolers, and Heat Recovery
Three Operational Modes			
Mode1 (Peak Summer)	Chillers only	RTES only	RTES only
Mode2 (Spring, Summer, and Fall)	Dry coolers and chillers	Dry coolers and RTES	Dry coolers, RTES, and heat recovery
Mode 3 (Winter)	Dry coolers only	Dry coolers only	Dry coolers and heat recovery
Supply Water Temperature	21 °C		

disadvantages. The RTES system is sustainable and reliable and consumes relatively less electricity compared to conventional cooling technologies, such as the chiller, to operate circulating pumps and dry coolers (for the seasonal recharging). However, the resource potential for an RTES system may vary significantly depending on climates, geologic settings, and physiography [23], and the RTES system possibly involves a high initial cost for drilling the RTES wells if the resource is available in deep formations. Although the capital and operational costs and electricity consumption for dry coolers are relatively low compared to those for the RTES and chillers, dry cooler operations are significantly affected by the ambient conditions, particularly dry bulb temperature. Inversely, capital and operational costs and electricity consumption for chillers are considerably higher than those for the RTES and dry coolers, but the chillers can supply the cooling load regardless of ambient conditions. Considering those characteristics, our design assumed that dry coolers have a priority for the data center cooling when available, and the remaining cooling loads not supplied by dry coolers are met either by a chiller in Scenario 1 (base case) or the RTES in Scenario 2 and Scenario 3. Even though the combinations of RTES, dry coolers, and/or chillers imply that each component typically operates at a capacity lower than its optimal design, potentially affecting performance, this study assumed that system operation is independent of any off-design performance. It is also important to note that configurations of the main heat rejection alternatives in actual data centers may vary significantly depending on design and operational conditions and should be thoroughly validated. While the three alternatives considered in this study are unique (and may be conceptual), the configuration designed here benchmarked the actual high-performance computing (HPC) data center at the National Renewable Energy Laboratory (NREL) in Golden, Colorado. In NREL's HPC data center, a combination of two different heat rejection alternatives—cooling towers and thermosyphons—reliably supply the cooling load, achieving a lower power usage effectiveness as mentioned in the introduction [14,15]. More details on the configurations of the three alternatives will be discussed in the next section, along with figures.

In addition to considering the advantages and disadvantages of heat rejection alternatives, the temperature of fluid circulating through the cooling system is crucial for designing the data center system [27,28]. The supply temperature for data center cooling may vary significantly depending on the demand during operation. However, for modeling purposes, this study assumed the supply temperature to be 21 °C based on the initial reservoir temperature of 17 °C, and 17 °C (W17) and 27 °C (W27) from the American Society of Heating, Refrigerating, and Air-Conditioning Engineers (ASHRAE) recommendations [29]. This study also assumed that 1) the fluid at 21 °C flows through the data center under a constant flow rate of 92 kg/s to supply the 5 MW cooling load, 2) the supply fluid temperature gains 13 °C throughout the ICT equipment and server racks in the data center, and 3) the approach temperature in heat exchangers for heat recovery and the RTES is 3 °C. Namely, the fluid temperature at 21 °C (that is, the first assumption) gains 13 °C through heat exchangers within the data center (that is, the third assumption) and becomes 34 °C at the outlet of data center heat exchanger. Water at 31 °C through heat exchangers in the RTES field (that is, the fourth assumption) was then injected into the RTES. Then, the RTES produced water at about 17.5 °C, which became about 20.5 °C through the RTES field heat exchanger for data center cooling.

Similarly, we assumed dry coolers supply water at a temperature of 6 °C higher than the ambient air temperature (that is, the approach temperature through dry coolers was assumed to be 6 °C). This implies that dry coolers had a full capacity to supply water at 21 °C for the data center cooling when ambient temperature was lower than 15 °C under varying flow rates depending on ambient temperature at the certain time step. However, our preliminary modeling results for the RTES 20-year performance demonstrated the RTES operations are thermally stable and balanced between charging and discharging of cold energy with the 10 °C threshold temperature, with respect to the targeted 21 °C supply water and subsurface temperatures. With the 10 °C threshold temperature, the RTES was utilized for supplying data center cooling load and storing cold energy during 48.1 % (summer) and 51.9 % (winter) of the year, respectively (Fig. 1). (See Table 1.)

For the heat recovery system in Scenario 3, our design assumed that 50 % of the thermal energy generated in the data center is recovered to supply water heating loads in the whole building during half the year. The temperature of 34 °C at the data center outlet decreased to 27.5 °C as the warm water flowed through the heat exchanger for heat recovery. Electricity consumption and costs for operating dry coolers and RTES in Scenario 3 decreased correspondingly due to the decreased cooling load (that is, flow rates of the fluid through the RTES and dry coolers decreased), while an additional heat exchanger, piping, and a circulating pump for the heat recovery were incorporated in the LCOC calculation. We also estimated and incorporated the revenue from heat recovery into the cost calculation. We assumed that a natural gas-fired boiler supplies the water heating load in the building, and operational costs of the boiler to supply the same amount of the recovered heating load was incorporated as the revenue. We used $12/mcf ($40.94/MWh) as the regional natural gas rate.

We optimized operational conditions of dry coolers in the three scenarios in terms of the approach, operational, and ambient temperatures to maximize the benefit of free cooling driven by fans (that is, ambient air utilization without refrigeration cycles) as briefly discussed earlier. In Mode 1, the RTES (or chillers in Scenario 1) supplies data center cooling when the ambient temperature is higher than 34 °C during the peak summer season (Fig. 2(a) and (b)). In Mode 2, the data center cooling load is supplied by both the RTES (or chillers in Scenario 1) and dry coolers when the ambient temperature is between 34 °C and 10 °C (Fig. 2(a) and (c)). In Mode 3, the dry cooler supplies cooling to the data center and recharges cooling capacity of the RTES when the ambient temperature is lower than 10 °C (Fig. 2(a) and (d)).

2.2. Reservoir thermal energy storage system modeling

We designed the RTES system in the Arapahoe aquifer hosted in the basal Arapahoe Conglomerate of the Denver Basin Group. The conglomerate is thickest near the Front Range (~100 m) and thins eastward toward the center of the basin. As shown in Fig. 3, the RTES is capped by confining units (shales and siltstones) of the D1 sequence (unit name of the Denver Formation) and underlain by low permeability shales and siltstones of the Cretaceous Laramie Formation [30]. The thickness of the RTES was estimated roughly as 350 ft. (107 m) near Golden at a depth ranging from 558 to 886 ft. (170–270 m) below ground surface [30]. Given the shallow depth of the targeted formation, low initial temperature, small temperature change, and fully saturated single-phase fluid flow were assumed for the system modeling.

The governing equation of mass and energy conservation can be expressed in terms of pore pressure P and temperature T (as)

$$\frac{1}{M}\dot{P} - A\dot{T} - \nabla\cdot\frac{\boldsymbol{\kappa}}{\mu_f}\left(\nabla P - \rho_f \boldsymbol{g}\right) = 0 \tag{1}$$

$$\frac{\partial \mathcal{E}}{\partial t} - \nabla\cdot\lambda\nabla T - \nabla\cdot\left(\rho_f C_f T\frac{\boldsymbol{\kappa}}{\mu}\left(\nabla P - \rho_f \boldsymbol{g}\right)\right) = 0 \tag{2}$$

where M is the Biot modulus, expressed in terms of porosity ϕ, fluid bulk modulus K_f, Biot coefficient α_B, and matrix (i.e., porous skeleton) bulk modulus K_m as $\frac{1}{M} = \frac{\phi}{K_f} + \frac{(\alpha_B - \phi)}{K_m}$. A donates the effective volumetric thermal expansion coefficient, calculated as $A = (1-\phi)\alpha_m + \phi\alpha_f$ with α_m, α_f denoting the volumetric thermal expansion coefficient of the porous matrix and the fluid, respectively. In addition, $\boldsymbol{\kappa}$ is the formation permeability tensor, μ_f, ρ_f represents the fluid viscosity and density, respectively. For the energy conservation equation, $\mathcal{E}$ is the energy density for the fluid-matrix system, calculated as $\mathcal{E} = (1-\phi)\rho_m C_m T + \phi\rho_f C_f T$, with ρ_m, C_m, C_f represents the matrix density, the specific heat of the matrix and the fluid, respectively. λ in Eq. 2 is the weighted thermal conductivity calculated as $\lambda = (1-\phi)\lambda_m + \phi\lambda_f$ and $\boldsymbol{g}$ is the gravity vector. The governing equations are solved using a fully coupled Finite Element Package – the PorousFlow module [32] in the Multiphysics Objective Oriented Simulation Environment (MOOSE) [33]. The MOOSE framework builds on the finite element library LibMesh and the solver library PETSc, which can solve multi-physics and multi-component problems in an implicit and parallel manner. The validation of MOOSE in modeling coupled heat transfer and fluid flow is provided in detail in [34].

The RTES system was modeled in a box with dimensions of 2000 m (length) × 1000 m (width) × 150 m (thickness). The model domain includes the caprock shale beds, Araphahoe aquifer, and basel shale beds, each with a thickness of 15 m, 105 m, and 30 m, respectively. A no-flux (undrained) boundary condition was applied to the top, bottom, and symmetrical surfaces, while a drain boundary condition was applied to the other sides with initial reservoir temperature of 16.5 °C [38] and initial hydrostatic pore pressure (linearly increase with depth) assuming the water table is at the surface (see Table 2 for the formation depth). Two 3D reservoir models were built first with layered or aquifer homogenous formations. The layered model divides the aquifer into 7 layers with a thickness of 15 m, while the homogeneous model treats the whole aquifer as a single layer with a thickness of 105 m (see the stratigraphic column in Fig. 3 or the same across the depth of the formation, respectively). The horizontal permeability of the homogenous model was set as 6.5×10^{-13} m^2 [35], while the horizontal permeability of each layer within the layered model was set randomly, but its average value is equal to 6.5×10^{-13} m^2 for comparison. For both models, their vertical permeability was set as 1 % or 10 % of horizontal permeability. We meshed the 2 model domains with hexahedron elements, and the horizontal element size varies from 2 m near the wellbores to 50 m in the boundary. In the vertical direction, a fixed 2-m element size was used. This mesh refinement captures the sharp gradient of pore pressure and the temperature. A separate 2D model, assuming a homogenous aquifer formation and ignoring the buoyancy effect and the heat conduction loss in the cap and base rocks, was also constructed to reduce the computational cost while maintaining prediction accuracy by comparing against the 3D model values. The 2D model is meshed with element size gradually changing from 2 m close to the wellbore to 50 me along the boundaries. A doublet system was designed in the model domain consisting of caprock, aquifer, and base-rock layers. Table 2 details the physical parameters of rock matrix obtained from literature and used for all the simulations. For the fluid related properties, we adopted the International Association for the Properties of Water and Steam-Industrial Formulation 1997 (IAPWS-IF97). In the RTES operation, warm water was injected into the hot well during summer to produce cold water for the data center cooling. During winter, warm water was extracted from the hot well to cool down the warm water using dry coolers and recharge the RTES using the cooled water. The system rests in the spring and fall seasons, and we performed a 2-year simulation for all the cases.

Fig. 4 compares example results for the heat plume around the hot well obtained from the two 3D modeling cases (homogenous or layered hydraulic properties) and one 2D modeling case at end of the first summer. While the 3D homogenous and 2D modeling cases showed similar results, the 3D layered case represented different sizes of heat plumes based on the different thermo-hydro-geological properties. Even though fluid temperature at the cold well of the 2D case showed 0.2 °C difference, there was no significant difference in the results obtained from the different cases (Fig. 3(c)). Pore pressures at the bottom of the two wells and average fluid temperatures within the two wells were identical despite the different range of heat plumes. The impact of the vertical-horizontal permeability ratio (κ_v/κ_h) in the two 3D modeling cases was also minimal. To optimize computational cost, we thus used

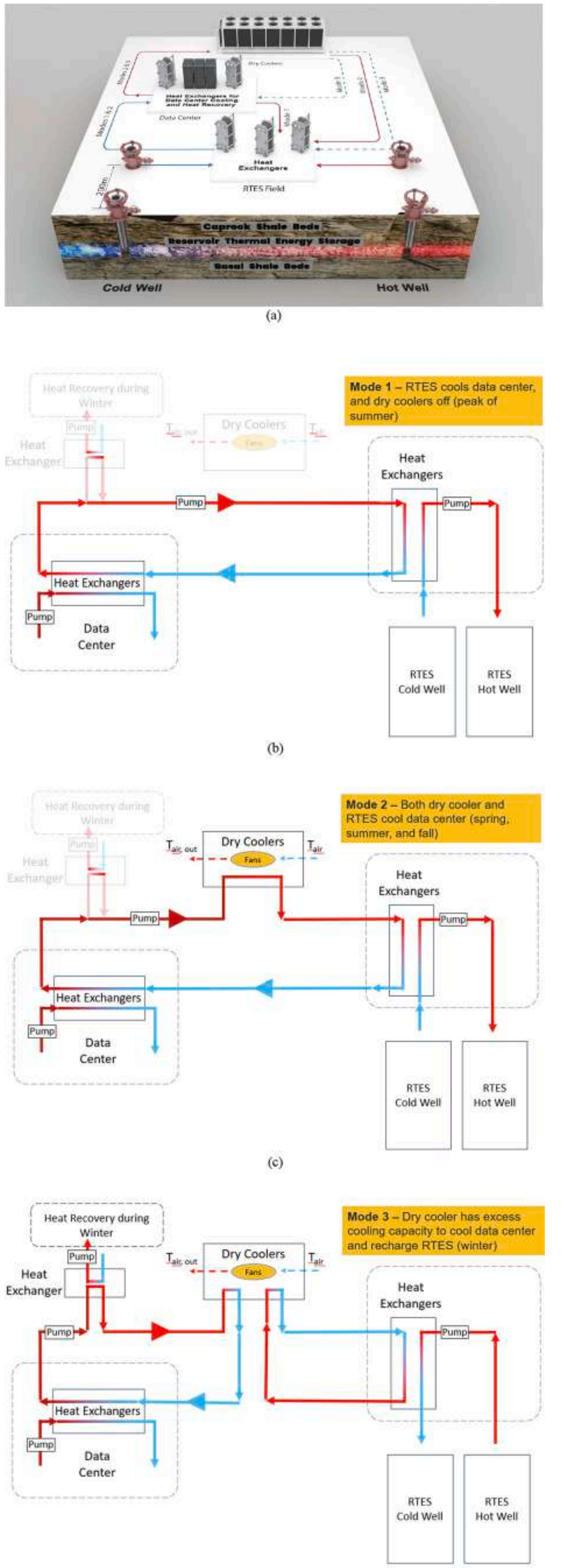

(caption on next column)

Fig. 2. RTES-based cooling systems for 5 MW data center in Golden, Colorado: (a) Overview of data center cooling system incorporated with reservoir thermal energy storage (or chillers in Scenario 1) in Mode 1. **(b)** Schematic of Mode 1. The RTES (or chillers in Scenario 1) solely supplies the data center cooling demand in Mode 1 when ambient temperature is higher than 34 °C. **(c)** Schematic of Mode 2. Both the RTES (or chillers in Scenario 1) and dry coolers supply the data center cooling in Mode 2 when ambient temperature is between 34 °C and 10 °C. **(d)** Schematic of Mode 3. Dry coolers are utilized to supply data center cooling demand and recharge the RTES in Mode 3 when ambient temperature is lower than 10 °C.

the 2D model domain for the 20-year RTES performance modeling with injection rates variably calculated for the targeted cooling energy production incorporated with dry cooler cooling for the 5 MW data center cooling load (see blue graph in Fig. 5). The maximum flow rates in Scenario 2 and Scenario 3 were 46 kg/s per a well at which the ambient temperature exceeded 34 °C and RTES was fully utilized to supply the 5 MW data center cooling load. Note that the amount of water flowed from the hot to the cold wells for data center cooling was approximately the same as the amount of water flowing from the cold to hot wells for RTES recharging, ensuring the sustainability of the RTES system.

2.3. *Levelized cost of cooling of the data center cooling system*

The LCOC is defined as a ratio of the system capital expenditures (CAPEX) and operational expenditures (OPEX) to cooling production over the system's lifetime (Eq. 3):

$$LCOC = \frac{C_{cap} + \sum_{t=1}^{LT} \frac{C_{O\&M,t}}{(1+d)^t}}{\sum_{t=1}^{LT} \frac{C_t}{(1+d)^t}} \tag{3}$$

where C_{cap} and $C_{O\&M}$ denote total up-front capital investment and annual average operations and maintenance cost, respectively; d is real discount rate, which was assumed to be 5 % in this study to address the present value of a future payment; t denotes time in year; LT stands for system lifetime (20 years); and C represents annual average cooling production. The levelized costs have been analyzed in the literature as an economic metric to compare the cost effectiveness of a system to those of different systems and/or production scenarios (e.g., [40,41]). We estimated the 20-year lifetime LCOC of the data center cooling systems connected to the RTES without heat recovery (Scenario 2) and with heat recovery (Scenario 3) and compared the LCOC to the LCOC of Scenario 1. While we excluded the cooling systems in the ICT equipment or server cabinets (e.g., immersion liquid cooling, CRAC, CRAH), the techno-economic analysis considered the main heat rejection alternatives, including dry coolers, chillers, and RTES, along with necessary components, such as pumps, distribution piping, and heat exchangers.

While assumptions for the maintenance costs varied depending on the components (see Section 2.3.2 for details), OPEX was estimated based on the electricity consumption of those key components. Specifically, the estimated electricity consumption was multiplied by two electricity rates, assumed as 1) 13.5 cents per kWh for the 12-h peak period (7:00 to 19:00) and 2) 9.5 cents per kWh for the 12-h off-peak period (19:00 to 7:00), reflecting a 2-cent increase above the average rate during peak hours and a 2-cent decrease during off-peak hours. In 2023, the average electricity retail price in Colorado was about 11.5 cents per kWh, which approximately aligns with the U.S. Energy Information Administration's (EIA) reported rate of 11.76 cents per kWh for the same year [42].

2.3.1. *Heat transfer rate in RTES and dry cooler system*

We estimated the rate of useful cooling energy delivered by RTES or dry coolers using Eq. 4:

$$Q = m \times C_p \times \Delta T \tag{4}$$

where Q is the heat transfer rate (W); m and C_p denote flow rate (kg/

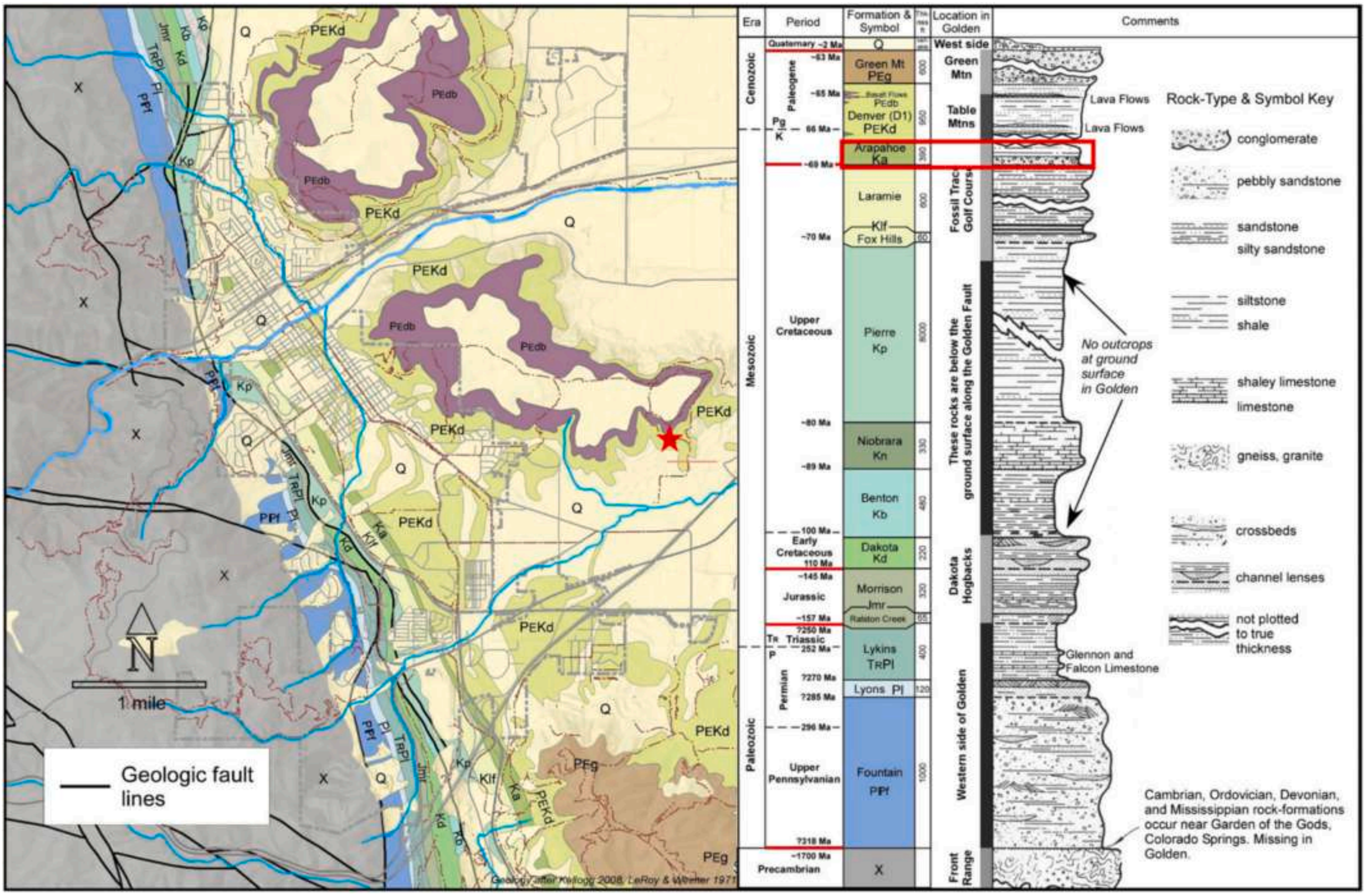

Fig. 3. Geologic map and stratigraphic column for the study area (modified after [31]). The red star in the geologic map indicates the location of the 5 MW data center. The Arapahoe Conglomerate formation targeted for the RTES is highlighted with a red rectangle in the stratigraphic column. (For interpretation of the references to color in this figure legend, the reader is referred to the web version of this article.)

Table 2
Physical parameter used in the simulation cases with values adopted from [35 – 39].

Parameter	Units	Domain		
		Caprock shale beds	Aquifer Arapahoe	Basal shale beds
Horizontal permeability, k_h	m^2	1×10^{-18}	6.5×10^{-13}	1×10^{-18}
Vertical permeability, k_v	m^2	$0.1/0.01k_h$		
Porosity, ϕ	–	0.01	34	0.01
Thermal expansion, α_m	1/K	1×10^{-5}		
Thermal conductivity, λ_m	W/(m K)	1.1	2.56	1.1
Specific heat, C_m	J/(kg K)	1000	920	1000
Grain density, ρ_m	kg/m^3	2500	2650	2500
Biot coefficient, α_B	–	0.8		
Bulk modulus, K_m	Pa	1.5×10^9		
Formation depth, H	m	155–170	170–275	275–375

s) and specific heat (J/kg·K) assumed as 4184.4 J/kg·K for water and 1005 J/kg·K for air; and ΔT represents a difference in temperatures at injection and production wells or inlet and outlet of dry coolers (°C). Variable flow rates of dry coolers were calculated for the targeted cooling energy production in terms of ambient temperature and the 6 °C approach temperature, while those of the RTES were estimated for the targeted RTES cooling production based on subsurface temperature obtained from the numerical modeling (Fig. 3).

2.3.2. Capital and operational cost estimations for key components

As represented in Fig. 2, we designed the data center cooling system with dry coolers, circulating pumps, heat exchangers, piping, and two hot and two cold wells (two doublets) for the RTES (Scenario 2 and Scenario 3), or chillers (Scenario 1). Key components considered in CAPEX and O&M or OPEX estimations were slightly different in each scenario: 1) Scenario 1 consisted of chillers, dry coolers, circulating pumps, heat exchangers, and an additional 100 m loop for chillers, 2) Scenario 2 consisted of two doublets with a bottomhole depth of 275 m for the RTES, dry coolers, two circulating pumps and two heat exchanger systems for each of the RTES and the data center loop, and piping of 700 m for the RTES field, respectively, and 3) Scenario 3 consisted of the same RTES configuration, dry coolers, three circulating pump and three heat exchanger systems for each of the RTES, the data center loop, and heat recovery, and piping of 700 m and 100 m for the RTES field and data center loop, respectively. In this study, we only considered the additional piping required for those key components in the three

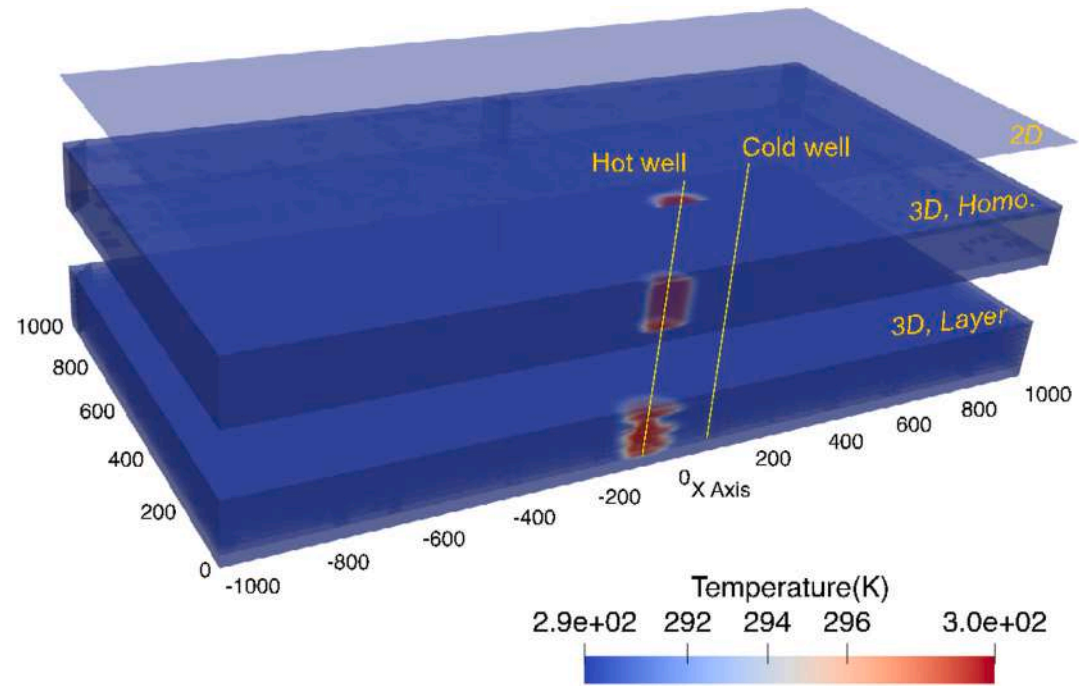

Fig. 4. Comparison of hot plume distribution at the end of first year summer among the 3D homogenous, layered, and 2D modeling cases. Note in the summer season, cold water was produced from the cold well for data center cooling and then reinjected back into the hot well.

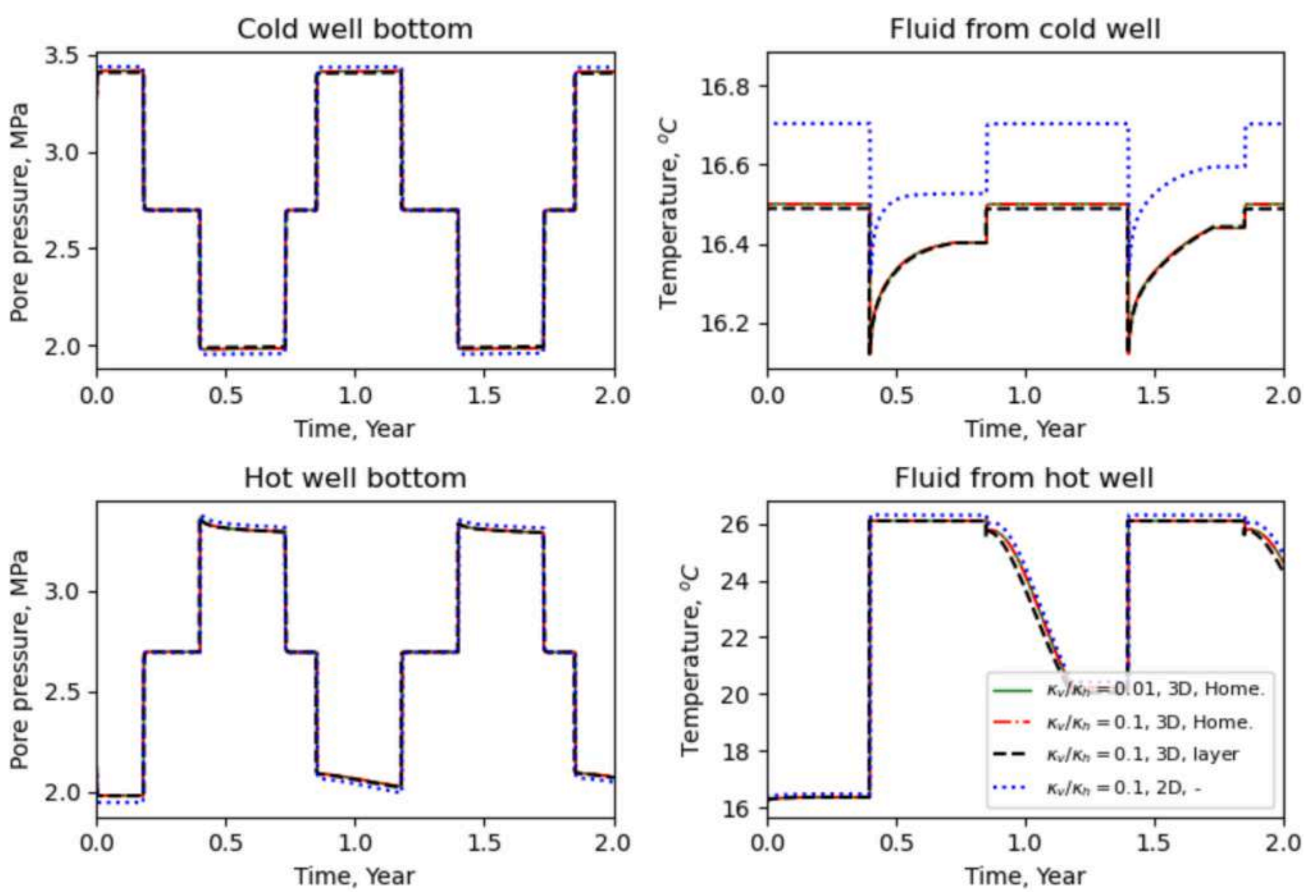

(c)

Fig. 5. Parametric modeling study to quantify the influence of 3D homogenous versus layered domain, vertical/horizontal permeability ratio, and 3D versus 2D model on RTES performance for a 2-year seasonal cycle operation.

scenarios, assuming that existing data center piping system could be utilized for the cooling systems with minimum retrofitting.

For estimating CAPEX of the key components, theoretical and empirical cost correlations (e.g., heat exchanger design based on heat exchange area) were initially collected from the literature review. The preliminary estimations were then validated through commercial market research, example projects, and discussions with industrial advisory group members. The estimations for some of the components were significantly lower than the U.S. market prices, and the cost correlations were subsequently calibrated or developed for this study (Table 3). It is important to note that the cost correlations may be valid for rough cost estimations of the components in the United States (2023 USD); however, separate validations are recommended for a specific case study before application.

The drilling cost was estimated using \$200/m (\$61/ft). To represent a typical drilling cost for shallow wells at a depth less than 1 km in Golden, Colorado, we interviewed regional drilling companies for the cost correlation and conducted a literature review (e.g., [43]). The \$200/m represents the cost from drilling to well completion. As demonstrated in Fig. 2(a), the RTES involved four wells with a bottomhole depth of 275 m. We assumed that the RTES wells are appropriately functioning without any issues during the system lifetime (that is, no maintenance cost).

For piping cost estimates, we surveyed piping companies and projects, including the piping cost estimate for the data center at the National Renewable Energy Laboratory in Golden, Colorado, and used \$754.6/m (\$230/ft) and \$519.8/m (\$158/ft) for piping in data center and the well field, respectively. We assumed the piping diameter is 10 in. (25.4 cm) and lengths are 100 m for each of the data center piping connected for chillers in Scenario 1 and heat recovery in Scenario 3 and 700 m for the RTES field consisting of 200 m connection piping between two cold wells or two hot wells and 300 m piping from the two wells to the heat exchanger (Fig. 2(a)). We also assumed that 3 % of the CAPEX approximately represents the annual maintenance cost, such as leaks, corrosion, checks for any signs of wear and tear, or repair, and it was assumed that piping is appropriately functioning without critical issues that require piping replacement during the system lifetime.

Plate and frame heat exchangers were designed for the data center, RTES, and heat recovery systems as represented in Fig. 2. Flow rates of the fluid flowing through the heat exchangers varied depending on the load and resource temperature, and we designed heat changers to supply any loads (that is, designed with the peak flow rate). To estimate CAPEX of the heat exchangers, we used \$2,221.1 per kg/s of flow rate (\$140/gpm) obtained from commercial market research that incorporates equipment and installation labor costs. We assumed that 5 % of the CAPEX approximately represents the annual maintenance cost, such as the cleaning to minimize fouling and scaling.

CAPEX of the pump used to circulate water through the data center loop was estimated using \$1000 per pump power (kWe), which is a typical market price in Colorado that addresses unit and installation labor costs. For pumps in the RTES wells, we used an empirical equation originally derived for production pump and driver in a single geothermal production well [44].

$$CAPEX_{pump} = \$1750 \times \left(P_{hp}\right)^{0.7} + \$5750 \times \left(P_{hp}\right)^{0.2} \times PPI_{pump} \tag{5}$$

where P_{hp} represents pump power in horsepower, converted from the pumping power (in watts) divided by 745.7. We used Eq. 6 to calculate the pumping power (in watts):

$$P_{pump} = \frac{q \times \Delta P_{wells\ or\ frictional}}{\eta} \tag{6}$$

where P_{pump} is the pumping power (W); q is the volumetric flow rate (m^3/s) estimated using the mass flow rate (kg/s) used in the numerical modeling for a specific amount of energy production or storage regarding the ambient temperatures, or a constant mass flow rate of 120 kg/s for the given 5 MW cooling load within the data center and water density of 997 kg/m^3 assumed as a constant in this study; η is the pump efficiency assumed as 80 %; and ΔP_{wells} is the pressure drop (Pa), obtained from the numerical modeling results. The pumping power on the data center side was calculated with frictional pressure drop ($\Delta P_{frictional}$) caused by a resistance to the fluid flow, the mass flow rates, 997 kg/m^3 fluid density, and 80 % efficiency. To calculate the $\Delta P_{frictional}$ throughout the data center loop, the Darcy friction factor was solved using the Darcy-Weisbach equation:

$$\frac{\Delta P_{frictional}}{L} = f_D \times \frac{\rho}{2} \times \frac{v^2}{D_H} \tag{7}$$

where L represents pipe length (m), which was the total additional pipe length for each of the heat rejection alternatives: 100 m in Scenario 1, 700 m in Scenario 2, and 800 m in Scenario 3. f_D and ρ are the Darcy friction factor and fluid density (kg/m^3), respectively. The mean flow velocity, v (m/s), was calculated with the flow rate, fluid density, and pipe specification. D_H represents the pipe hydraulic diameter (m). We also calculated the pumping OPEX using the pump energy in kilowatt-hours converted from the pump power in kilowatts by multiplying the operational hours with regional peak and off-peak rates of \$0.135/kWh

Table 3
Summary of cost correlations and assumptions for estimating CAPEX of key components in three scenarios.

	Scenario 1	Scenario 2	Scenario 3
Drilling			
Depth (m)	N/A	275	
Cost Correlation	N/A	\$200/m	
Piping			
Diameter (cm)	25.4		
Length in RTES Field (m)	N/A	700	700
Cost Correlation	N/A	\$519.8/m	
Length in Data Center (m)	100	N/A	100
Cost Correlation	\$754.6/m	N/A	\$754.6/m
Heat Exchanger			
Cost Correlation	\$2,221.1 per kg/s of flow rate (\$140/gpm)		
Circulating Pump			
Cost Correlation for Data Center Pump	\$1000/kWe		
Cost Correlation for RTES Pump	N/A	$CAPEX_{pump} = \$1750 \times \left(P_{hp}\right)^{0.7} + \$5750 \times \left(P_{hp}\right)^{0.2} \times PPI_{pump}$ [44]	
Chiller			
Cost Correlation	\$800/ton	N/A	N/A
Dry Cooler			
Electricity Consumption	0.25 kWe per kg/s of air flow rate [45]		
Cost Correlation	\$1066/kWe [46]		

and \$0.095/kWh, assuming peak and off-peak times are from 7:00 to 19:00 and from 19:00 to 7:00, respectively. PPI_{pump} is a producer price index to adjust cost to the year for which the estimation is being performed, which was 1.47. We assumed that 3 % of the CAPEX approximately represents the annual maintenance cost, such as leaks, corrosion, checks for any signs of wear and tear, or minor repair, assuming the pumps are fully functioning for 15 years. We calculated and incorporated replacement cost for the RTES pumps using the first and third terms in Eq. 5, $\$1,750 \times (pump\ hp)^{0.7} \times PPI_{pump}$, assuming the pump and driver are replaced every 15 years.

Chillers were designed for Scenario 1 in Mode 1 and Mode 2 where dry coolers cannot supply 100 % of the data center cooling load. The chiller CAPEX was estimated using a cost correlation of \$800/ton obtained from commercial market research. The peak electricity consumption was 2.13 MWe for the CAPEX estimation, and the variable power consumptions were incorporated with the operational hours for OPEX calculations. While the OPEX was calculated using the regional peak and off-peak rates, we assumed that 8 % of the CAPEX approximately represents the annual maintenance cost.

For dry cooler CAPEX and OPEX, we first estimated varying air flow rates of dry coolers using Eq. 4. The variable delta temperatures (ΔT) and desired cooling loads (Q) at hourly intervals were calculated with the 6 °C approach temperature we assumed, ambient temperature profile in Fig. 1, and the full 5 MW or the rest of cooling loads (where chillers in Scenario 1 or the RTES in scenarios 2 and 3 did not supply). Then, we estimated the electricity consumption of the dry coolers using an empirical correlation of 0.25 kWe per kg/s of the air flow rate, assuming the parasitic power to run the fans in dry coolers is very nearly constant [45]. The CAPEX of dry coolers was then estimated using a cost correlation of \$1066/kWe [46]. Similar to the pumping OPEX calculations, the power was converted to energy in kilowatt-hours, and the dry cooler OPEX was calculated with the peak and off-peak rates. We assumed that 5 % of the CAPEX approximately represents the annual maintenance cost.

2.4. CO_2 emissions

Electricity is a secondary energy source generated from primary energy sources such as fossil fuels, nuclear energy, and renewable energy resources [47]. Electricity generation, especially from burning

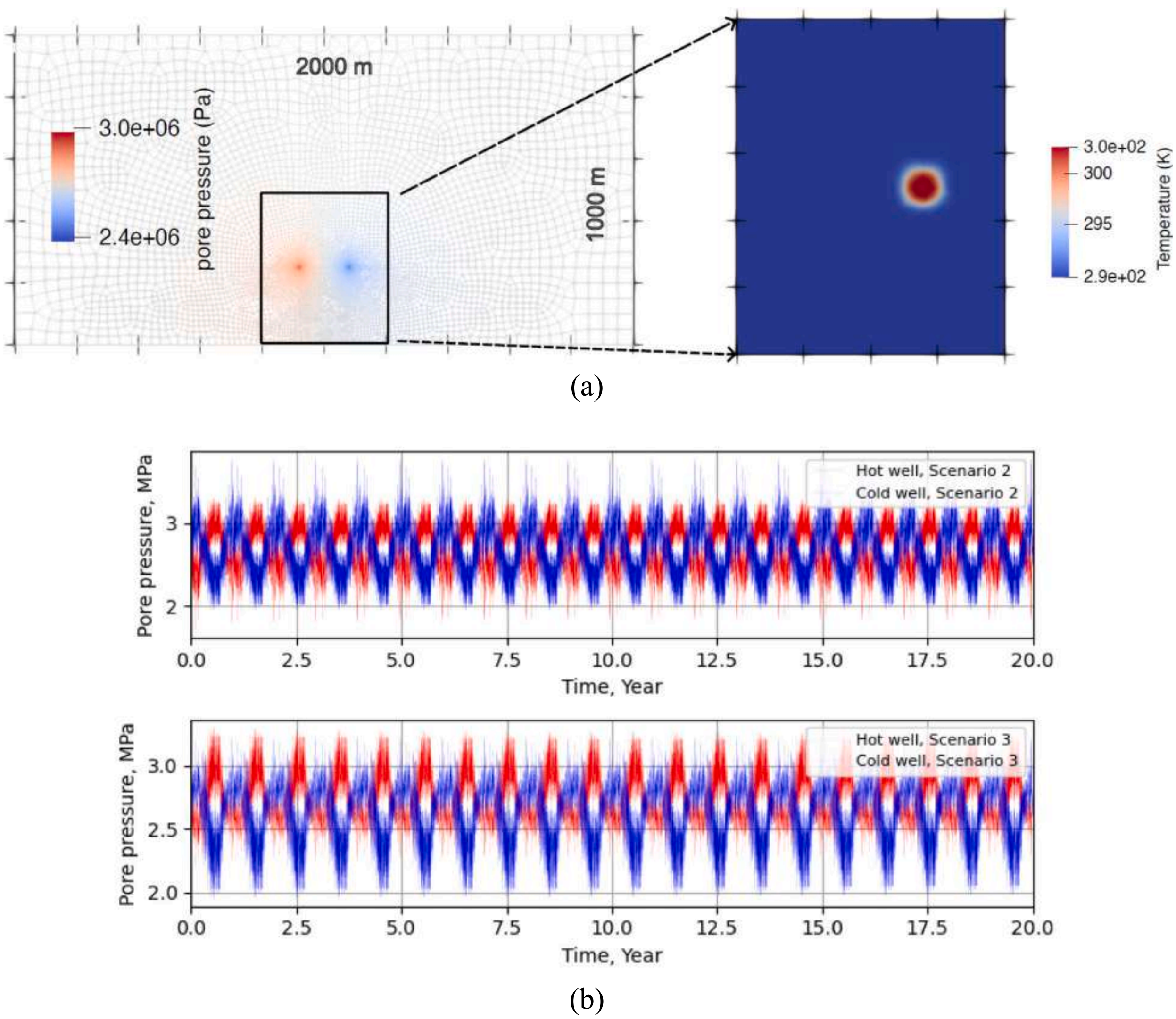

Fig. 6. 20-year performance of the reservoir thermal energy storage system for data center cooling. (a) Predicted pore pressure distribution (left) and temperature distribution (right, zoomed in region of wells) for Scenario 2 with two doublets. Note that only one doublet was simulated by leveraging the symmetry condition. **(b)** Predicted pore pressure in the hot and cold wells. **(c)** Predicted fluid temperature in hot and cold wells. **(d)** Cooling capacity of the RTES throughout 20 years of operation.

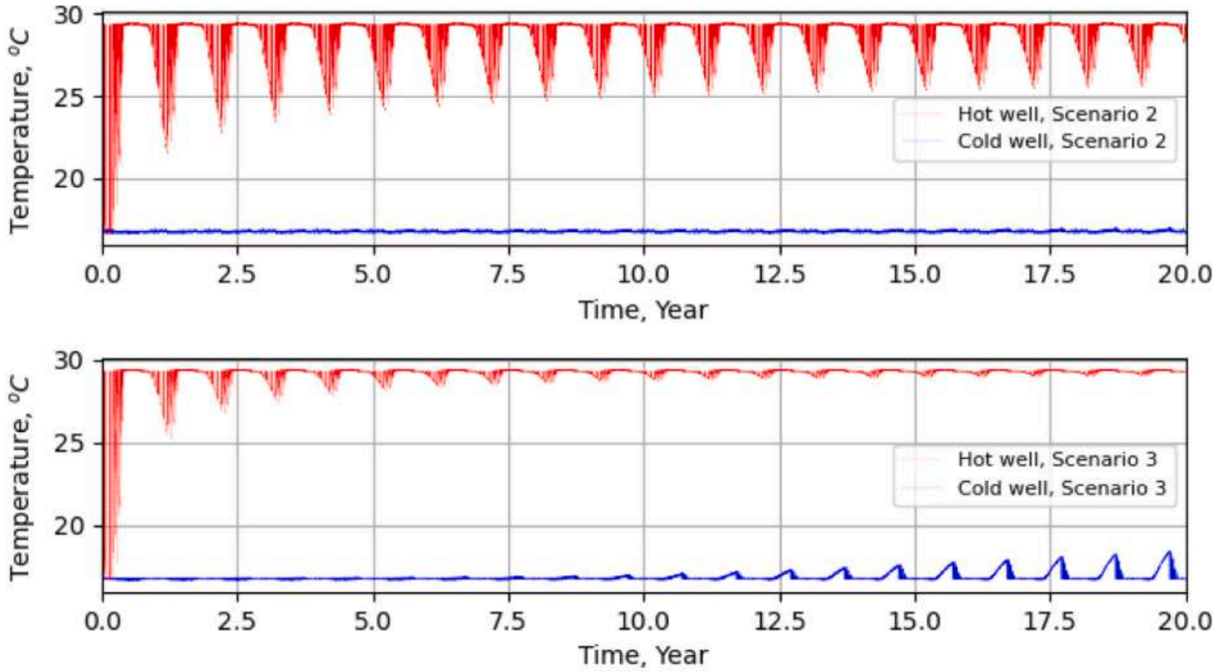

(c)

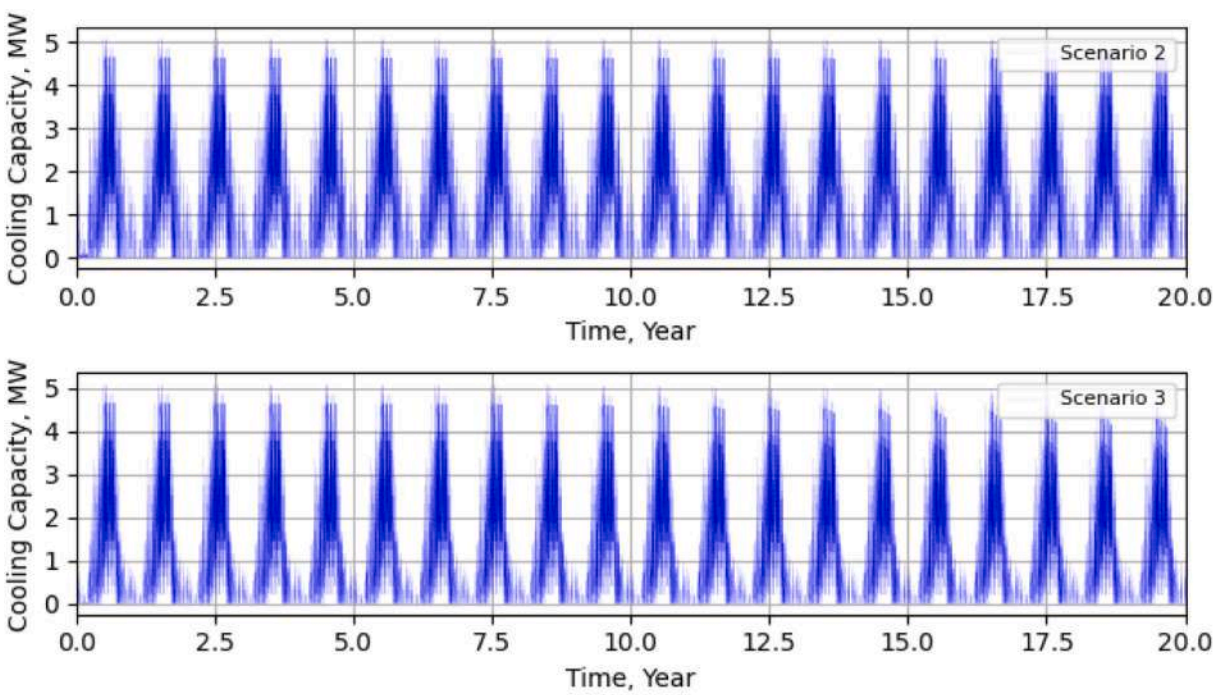

(d)

Fig. 6. (*continued*).

fossil fuels, involves a substantial amount of CO_2 emissions [48,49]. The emissions factor, which is a factor to convert activity data to greenhouse gas emissions, has often been used to quantify the gas emissions [50,51]. The EIA publishes emissions factors every year for each state to estimate the amount of certain gases released when electricity is generated by burning fossil fuels. To estimate the CO_2 emissions from operations of the three cooling systems, we used the EIA's emissions factor for Colorado, 1127 lb./MWh (0.51 t/MWh). We also estimated the CO_2 emissions from natural gas-fired boilers for the 2.5 MW of thermal energy recovered for water heating in Scenario 3 using 0.2 lb./MMBtu [52].

3. Results

3.1. Long-term performance of RTES system for data center cooling

Fig. 6(a) shows the simulated pore pressure distribution in the 2D simulation domain and temperature distribution in the zoomed-in area close to the doublet wells when RTES was charged during the winter. The pressure-disturbing zone was much larger (that is, relatively greater gradient in a larger area) than the plume of the hot fluid (that is, relatively smaller gradient), which is the reason that a 2 km domain was considered in the simulation. Maximum (red color) and minimum (blue color) pore pressures mark the locations of the two wells, and the well pressures were dynamically evolving with respect to operational schedules of different scenarios. The maximum and minimum well pressures switched back and forth with a change in the direction of injection and extraction. The size of the hot fluid plume also changed with respect to the injection plan, and its maximum size was within one-half the doublet distance to ensure no thermal breakthrough. Fig. 6(b) presents the predicted pressure evolution at the two wells across 20 years of operation. The maximum pressure difference between the cold and hot wells was approximately 2 MPa and 1.5 MPa in Scenario 2 and Scenario 3, respectively. This is because the heat recovery system in Scenario 3 reduced the cooling loads and consequently the injection and production flow rates. The fixed RTES annual operation in Mode 1 and Mode 2 dictated well pressure evolution manifests as a perfectly repeated pattern year by year. However, the temperature of the fluid extracted from the hot well during the RTES recharging period increased over time and converged to 29.5 °C (Fig. 6(c)). The cold well temperature in Scenario 3 also slightly increased after the 10-year operation due to the imbalanced cold energy injection and extraction. Nonetheless, the RTES cooling capacity was consistently maintained throughout the 20-year operation time (Fig. 6(d)). The energy imbalance can be minimized by increasing the cold water injection rate or temperature during winter, or by increasing the reservoir size.

3.2. Levelized cost of cooling for data center cooling systems

Table 4 summarizes the annual average rate of useful cooling energy delivered by RTES, dry coolers, chillers, or heat recovery, and system costs for the three cooling scenarios. The RTES supplied the data center cooling for 4214 h (48.1 % of the year) while the dry coolers supplied the data center cooling load with different utilization percentages during the whole year except 12 h in Mode 1. In Scenario 1 and Scenario 2, dry coolers supplied 3.2 MW cooling load on average during spring, summer, and fall in Mode 2 (4202 h), and the rest of the 1.8 MW cooling load was supplied by chillers or the RTES for the full 5 MW data center cooling load. Dry coolers solely supplied the 5 MW cooling load during winter in Mode 3 (4546 h). During the winter, dry coolers also supplied cooling of 1.6 MW and 1 MW on average to recharge the RTES in Scenario 2 and Scenario 3, respectively (up to 5.1 MW and 3.5 MW, respectively). In Scenario 3, operations of the RTES and dry coolers were generally reduced with respect to the heat recovery of an average of 0.4 MW in Mode 2. During the winter in Mode 3, 2 MW of thermal energy was recovered on average, and dry coolers solely supplied 3 MW cooling load without the RTES.

Total CAPEX for the cooling systems was $1.41 million on average, and chillers in Scenario 1 had the highest CAPEX among the components (Fig. 7(b)). Although drilling and additional dry coolers, piping, circulating pumps, and heat exchangers were included for capital cost calculations in the two RTES scenarios, the total CAPEX related to the RTES system was lower than the chiller CAPEX. Fig. 7(d) and (f) show that the heat exchanger CAPEX was the highest in the two RTES scenarios, particularly in Scenario 3, because the heat exchanger size increased for heat recovery. Dry cooler CAPEX varied depending on the operational conditions of chillers or the RTES, and dry cooler CAPEX in Scenario 1 was higher than that in the two RTES scenarios (see yellow portions in Fig. 7(a)). This is because we designed the RTES to produce the cooling slightly above 5 MW (Mode 1) or the variable cooling loads combined with dry coolers (Mode 2) due to uncertainties in the subsurface conditions (that is, dry cooler operations reduced by the additional RTES cooling production) while chillers and dry coolers in Scenario 1 accurately produced the desired cooling in terms of the ambient temperature.

Similar to the higher CAPEX for chillers, the OPEX for chillers in Scenario 1 was significantly higher than the OPEX for any other components in the three scenarios and was the key driver for an increase in LCOC in Scenario 1. Cho et al. [53] also highlighted the economic performance of data center cooling systems was critically affected by the usage of chillers. The chiller-based Scenario 1 showed the highest LCOC of $15/MWh among the three scenarios. Although we designed the chillers to have variable coefficients of performance (COP) ranging from 2.3 to 3.1 depending on the ambient and desired temperatures and cooling loads, the chillers still consumed a significant amount of electricity (that is, higher operational cost) to supply the targeted cooling loads (Fig. 7(c)). On the other hand, the RTES consumed a relatively small amount of electricity for circulating pumps to supply the cooling loads, even though dry coolers were utilized to recharge the RTES during the winter (Fig. 7(e) and (g)). Correspondingly, the 20-year lifetime LCOC significantly decreased with the RTES systems to $5.7/MWh in Scenario 2 and $5/MWh in Scenario 3. Of the two RTES scenarios, the OPEX in Scenario 3 was lower primarily due to the reduced RTES operations. These results imply that the additional pumping cost for heat recovery in Scenario 3 was relatively insignificant compared to the RTES pumping cost. In addition, the revenue from heat recovery, which takes about 21.3 % of the annual operational cost, further decreased the annual cash flow.

The LCOC of $5.7/MWh and $5/MWh for the two RTES-based data center cooling systems are lower than the LCOC of data center cooling systems reported in the literature, as well as the base case in this study. Liu et al. [54] designed a liquid air-based immersion cooling system for a 10 MW data center cooling load and estimated the optimal LCOC of the cooling system at $0.245/MJ, which is approximately equivalent to $882/MWh. In contrast, Alipour et al. [55] estimated the LCOC of a data center cooling system integrating a solar parabolic collector and a two-effect absorption chiller at $0.05815/kWh, or approximately $58.15/MWh. Due to variations in system components, configurations, and economic models across the studies including this study, the estimated

Table 4
Cooling production, electricity consumption, and levelized costs of data center cooling system.

Mode	Scenario 1	Scenario 2	Scenario 3
	Annual Average Rate of Useful Cooling Energy Delivered (MW)		
Mode 1 (Peak Summer)	5 by chillers	5 by the RTES	5 by the RTES
Mode 2 (Spring, Summer, and Fall)	3.2 by dry coolers and 1.8 by chillers	3.2 by dry coolers and 1.8 by the RTES	2.9 by dry coolers, 1.7 by the RTES, and 0.4 by heat recovery
Mode 3 (Winter)	5 by dry coolers	5 by dry coolers	3 by dry coolers and 2 by heat recovery
Annual Electricity Consumption			
Electricity Consumption (GWh/yr)	3.7	1.1	0.8
Levelized Cost of Cooling			
LCOC ($/MWh)	15	5.7	5

LCOC differs significantly. Nonetheless, these findings suggest that the LCOC of data center cooling systems can be optimized through technical and economical designs, facilitating adoption across various scales and operational contexts (e.g., regional climate conditions, grid costs).

3.3. Impact of the RTES-based data center cooling system on environment

Fig. 8 compares electricity consumption and CO_2 emissions in the three cooling scenarios. Annual total electricity consumptions for the three scenarios were 3.72 GWh/yr, 1.1 GWh/yr, and 0.81 GWh/yr, respectively. When compared to Scenario 1, Scenario 2 and Scenario 3 annually saved 2.6 GWh (70.3 % reduction) and 2.9 GWh (78.2 % reduction) of electricity, respectively (Fig. 8(a)). The electricity consumption for chillers in Scenario 1 was 2.8 GWh/yr (75.6 % of the annual total), which was much higher than the electricity consumption for any other components. The electricity consumption in Scenario 1 was dependent on the ambient temperature and was significant, especially during the summer when dry coolers have limited capacity for the data center cooling (Fig. 8(a)). In contrast, electricity consumption in the two RTES scenarios was relatively consistent and identical during the summer. The heat recovery in Scenario 3 saved 36.2 kWh on average during the winter season compared to Scenario 2.

In addition, we calculated electrical peak loads for each scenario, combining electricity consumptions for 1) chillers (Mode 1 and Mode 2 in Scenario 1), 2) pumps, 3) dry cooler used for partial (Mode 2) or full (Mode 3) data center cooling, and 4) dry cooler used to recharge the RTES (Mode 3) at the same time step. The peak loads for Scenarios 1–3 were 2132.2 kWh, 211.7 kWh, and 108.6 kWh, respectively. The peak load in Scenario 1 was solely from the chiller operation when the ambient temperature was the highest at 36 °C (that is, the greatest delta temperature between ambient and desired). The peak load in Scenario 2 was observed in Mode 3 when dry coolers supplied both the data center cooling and RTES recharging loads, whereas the peak load of 108.6 kWh in Scenario 3 occurred when the ambient temperature was as high as 32 °C in Mode 2. This result implies that the heat recovery in Scenario 3 brings a benefit to reduce peak load as well as the annual electricity consumption total.

We also estimated CO_2 emissions from the data center cooling system

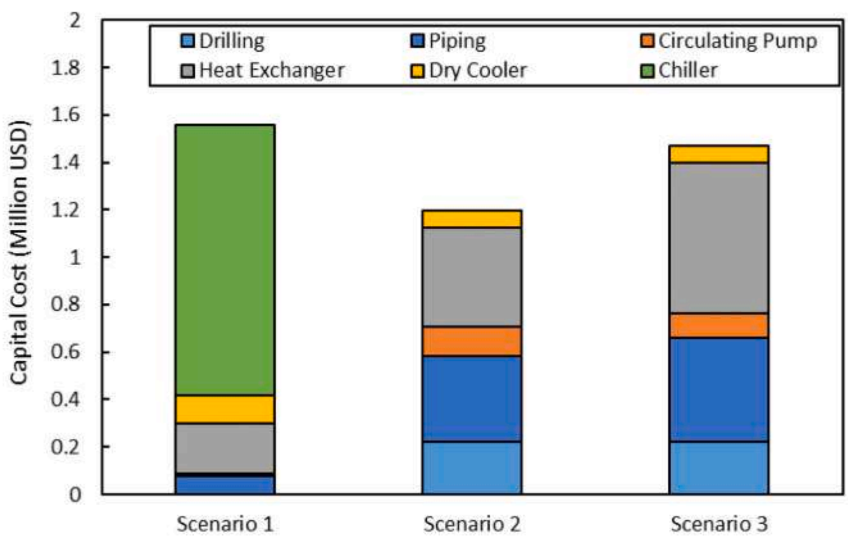

(a)

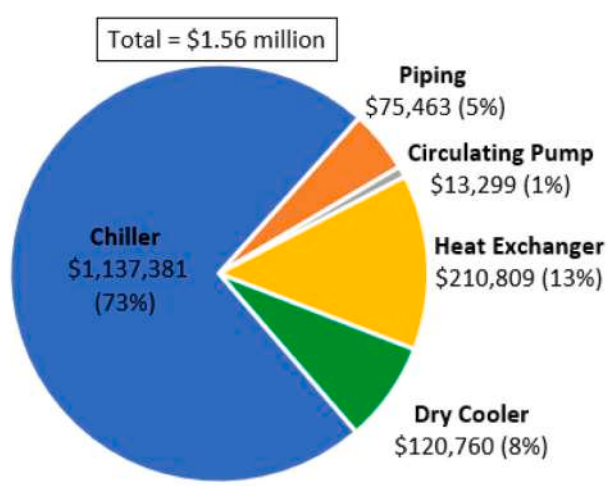

(b)

Fig. 7. Costs of the data center cooling systems in the three scenarios. (a) Capital costs for each component in the three scenarios. **(b, d, f)** Percentage shares and CAPEX for each component in three scenarios. **(c, e, g)** Percentage shares and OPEX for each component in three scenarios. Note that the heat recovery in Scenario 3 (g) annually saves about $20 k in the total operational cost.

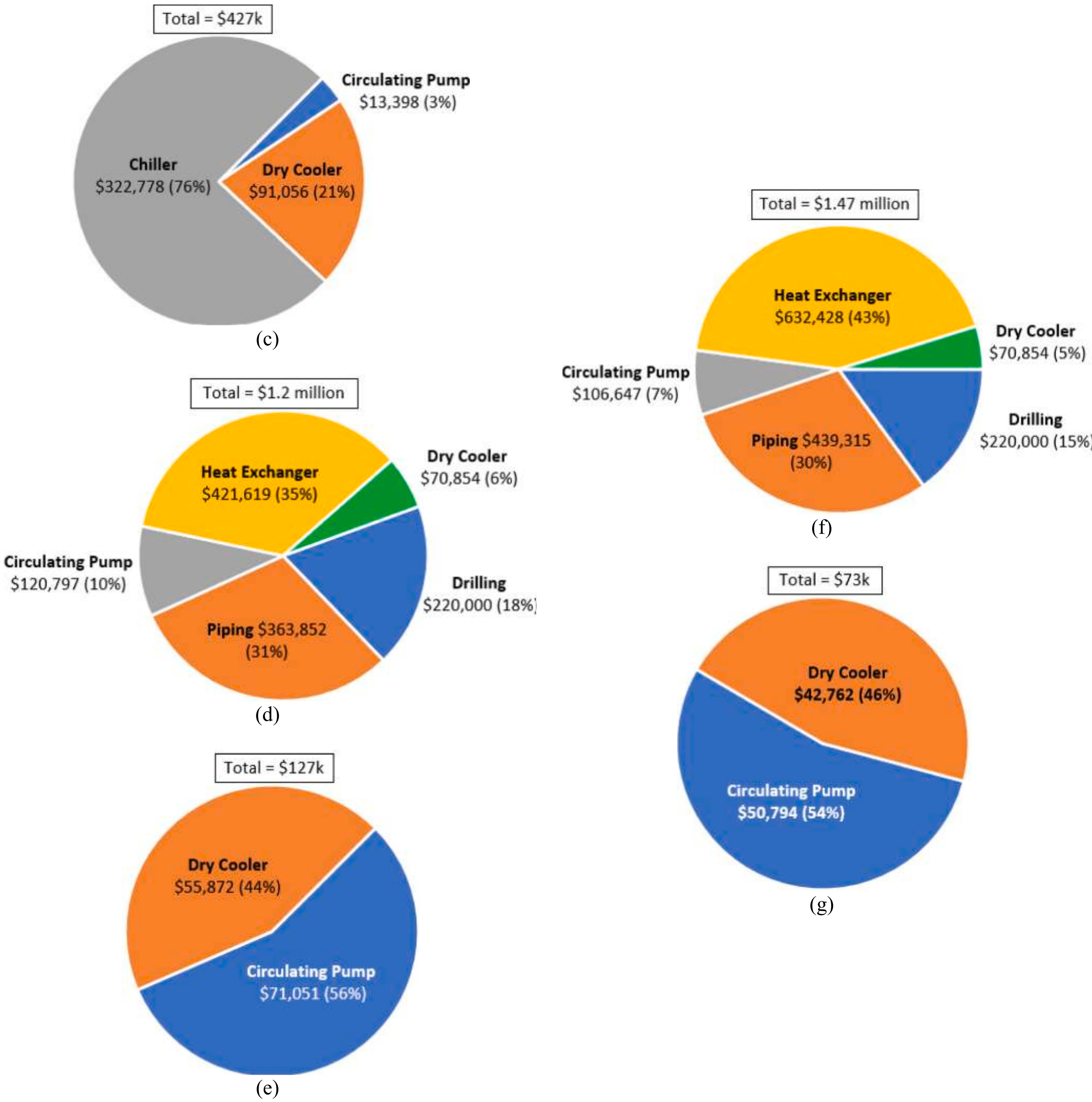

Fig. 7. (*continued*).

operations using the EIA's emissions factor for Colorado and the annual electricity consumption data we calculated above. Proportional to the electricity consumption, Scenario 1 showed significantly higher CO_2 emissions of 1898.8 tCO_2e than Scenario 2 of 564.1 tCO_2e and Scenario 3 of 413.9 tCO_2e (Fig. 8(b)). In other words, 1334.7 tCO_2e and 1488.3 tCO_2e emissions can be avoided with the two RTES scenarios (70.3 % and 78.2 % decreases by Scenario 2 and Scenario 3, respectively).

4. Discussion

Although we demonstrated that the RTES supplies the data center cooling load in a sustainable, economical, and environmentally friendly manner compared to the base scenario, the performance of RTES systems may vary significantly due to different subsurface conditions in the specific study area at a certain depth. For example, the RTES capacity may not be sufficient with the two doublet wells for the 5 MW cooling load due to an unexpectedly higher subsurface temperature. In this case, the flow rate should be increased to achieve the desired load, or the RTES pre-cooling process may be considered for decreasing initial subsurface temperature before use. However, water injection into the RTES with the increased flow rates can create fractures in the targeted formation (even injection-induced seismicity can occur), especially when the RTES pressure increased by the water injection is higher than the fracturing pressure under given in situ stress conditions, and thus additional wells may be needed for the optimal flow rate, such as maximum 92 kg/s designed for the specific conditions in this study.

To address what could happen if subsurface temperatures are higher than expected, requiring additional well drilling, pumping, dry cooler, and piping system capacity, we estimated the LCOC of the two RTES cooling scenarios that have four-doublet systems (that is, two additional

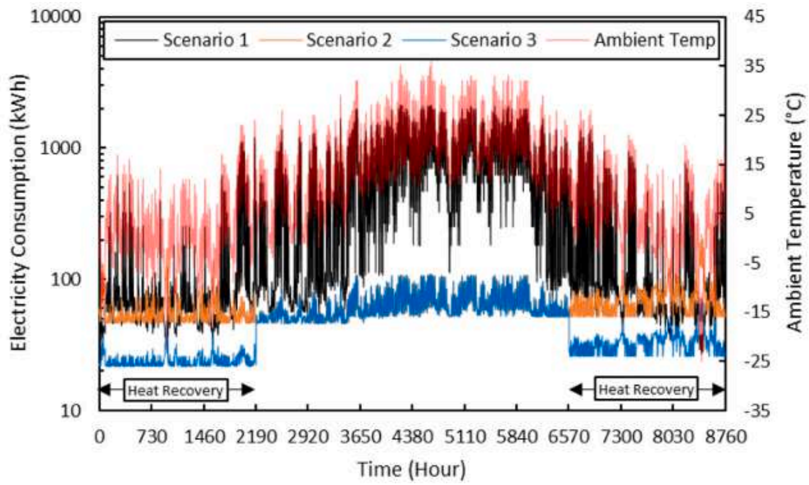

(a)

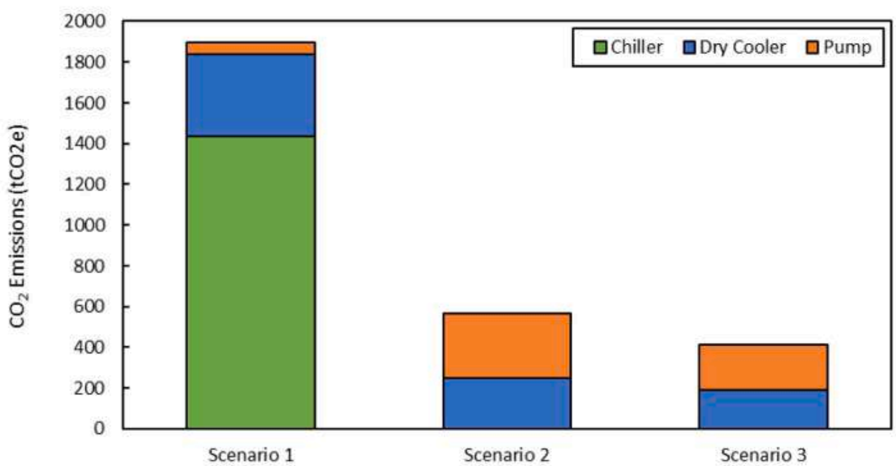

(b)

Fig. 8. Electricity consumption and CO_2 emissions in the three scenarios. (a) Electricity consumption profiles for the three scenarios. The RTES-based cooling systems can save 2.6 GWh (70.3 % reduction) without heat recovery in Scenario 2 and 2.9 GWh (78.2 % reduction) with heat recovery in Scenario 3. **(b)** Annual CO_2 emissions from component operations in the three scenarios.

doublets), which are the worst-case scenarios in terms of the system costs. With the four doublet systems, the CAPEX increased by 18.4 % in Scenario 2 and 15 % in Scenario 3. The 20-year lifetime O&M cost increased by 43 % in Scenario 2 and 39.2 % in Scenario 3, respectively (Fig. 9(a)). Although the LCOC correspondingly increased from $5.7/MWh to $6.1/MWh in Scenario 2 (6.7 % increment) and from $5/MWh to $5.4/MWh in Scenario 3 (7.7 % increment), the increased LCOC of the two RTES scenarios remained significantly than the base case LCOC of $15/MWh. Despite the higher system costs associated with additional wells, it is important to note that these wells enhance operational flexibility (e.g., enabling reduced operation during peak hours or seasons), which could benefit the electric grid.

Similarly, there are uncertainties in the system cost calculations with respect to escalated electricity rates that can significantly affect both OPEX and LCOC, notably in Scenario 1. Here, we calculated lifetime system cost and LCOC of the three cooling scenarios with the peak and off-peak rates increased by 20 % or decreased by 10 %. Fig. 9(b) shows that changes in the LCOC with the rates were sensitive particularly in Scenario 1 (6.5 % decrease at 10 % decreased rate and 13 % increase at 20 % increased rate), because of the greater amount of electricity consumption by chillers. The LCOC in the two RTES scenarios increased by 10.2 % and 10.4 % at the 20 % increased rate, respectively, and decreased by 5.1 % and 2.5 % at the 10 % decreased rate, respectively. That is, increases in the LCOC associated with 20 % increased rate (10.2 % and 10.4 %) were more significant than the LCOCs increased by a doubled system size (6.7 % and 7.7 %). Note that electricity rates along with regionally varying peak and off-peak hours (i.e., rates for peak and off-peak periods) may change differently over time, as may the rates themselves, depending on energy demand and market conditions. Even though this study assumed electricity rates with a 4-cent difference between 12-h peak and off-peak periods, future research is suggested to investigate regional electricity rate structures, grid costs, and their projections (e.g., capacity expansion models), which can vary significantly based on local consumption patterns and providers, and to further optimize operational conditions of the data center cooling systems in relation to these factors.

We also extended the LCOC calculations for a 50-year lifetime, as the RTES we designed showed reliable performance for 5 MW cooling production during summer periods for 20 years (Fig. 6). In the literature [38,56], the analysis on levelized costs for geothermal energy systems often considered a lifetime of 20 to 50 years. With the increased system lifetime, the RTES cooling production slightly decreased (approximately 1 %), while we assumed Scenario 1 produces the same cooling energy during the 50-year lifetime. Despite increases in the lifetime OPEX (approximately 47 %), the LCOC generally decreased from $15/MWh to $14.1/MWh (5.7 % decrement) in Scenario 1, from $5.7/MWh to $5/MWh (12.8 % decrement) in Scenario 2, and from $5/MWh to $3.6/MWh (27.9 % decrement) in Scenario 3 (Fig. 9(c)). The greatest reduction in the LCOC of Scenario 3 was primarily due to a relatively lower operational cost (that is, a lower impact from the increased operational time). These results indicate that the RTES-based cooling system becomes more cost-effective over time due to the lower annual operational costs. However, it is important to note that long-term operation of the RTES system can encounter various operational and maintenance challenges, which were not considered in this study, potentially stemming from both the natural environment and the system components, such as clogging, fouling, or corrosion of piping.

Lastly, similar to the impact of escalated electricity rate on the cost estimation, the system cost could be affected by the assumptions we made. For example, the cost correlation of $800/ton used to estimate the chiller CAPEX, which took about 73 % of the total CAPEX in Scenario 1 (Fig. 7(b)), may vary depending on the manufacturer, design specifications, and the system size. We selected four key drivers affecting system costs in the three scenarios (see the pie charts in Fig. 7), and the upper and lower bounds were set for the sensitivity analysis to reflect typical market price in the United States: chiller CAPEX ranging from $500/ton to $1400/ton, data center piping CAPEX ranging from $160/ft. to $300/ft., well field piping CAPEX ranging from $100/ft. to $350/ft., heat exchanger CAPEX ranging from $80/gpm to $200/gpm, and discount rate ranging from 10 % to 2 %. The results in Fig. 9(d–f) demonstrate that the LCOC can range from $11.5/MWh to $18.4/MWh in Scenario 1, from $4.7/MWh to $6.8/MWh in Scenario 2, and from $4.3/MWh to $6/

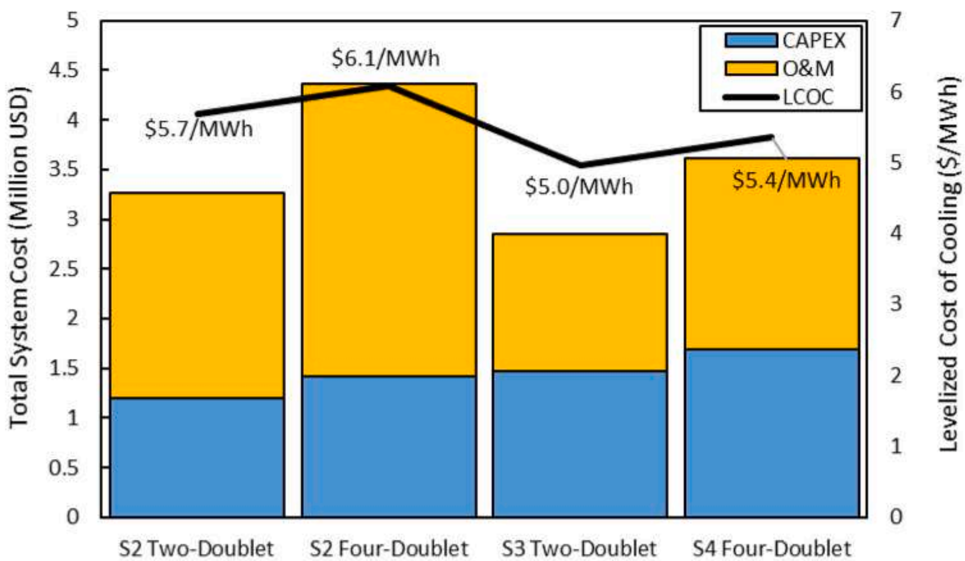

(a)

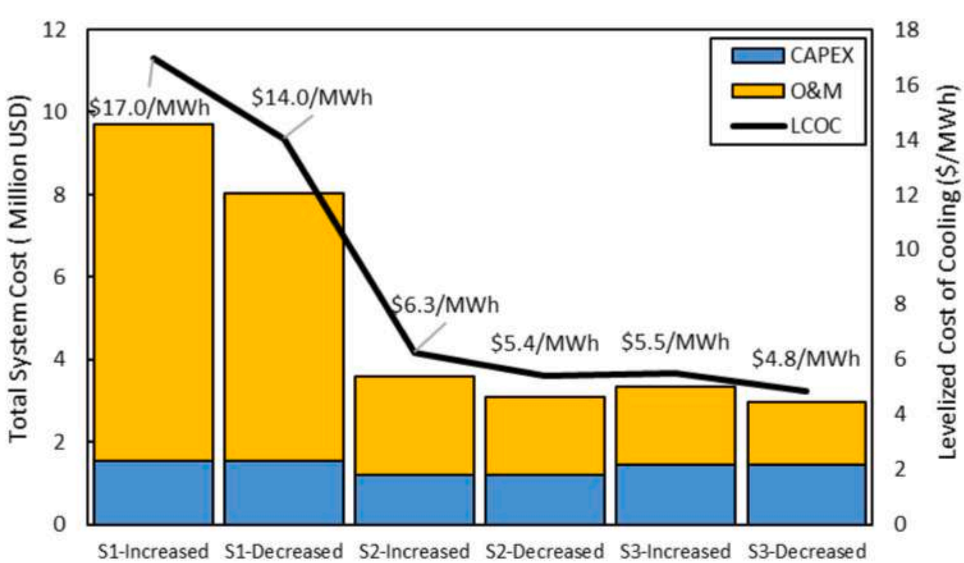

(b)

Fig. 9. Sensitivity analysis. (a) Total system cost and levelized cost of Scenario 2 and Scenario 3 with two different RTES system sizes. **(b)** Total system cost and levelized cost of each scenario with 20 % increased and 10 % decreased electricity rates. **(c)** Total system cost and levelized cost of each scenario with 20-year and 50-year system lifetime. **(d, e, f)** Percentage decrease or increase in the LCOC of Scenario 1, Scenario 2, and Scenario 3, respectively.

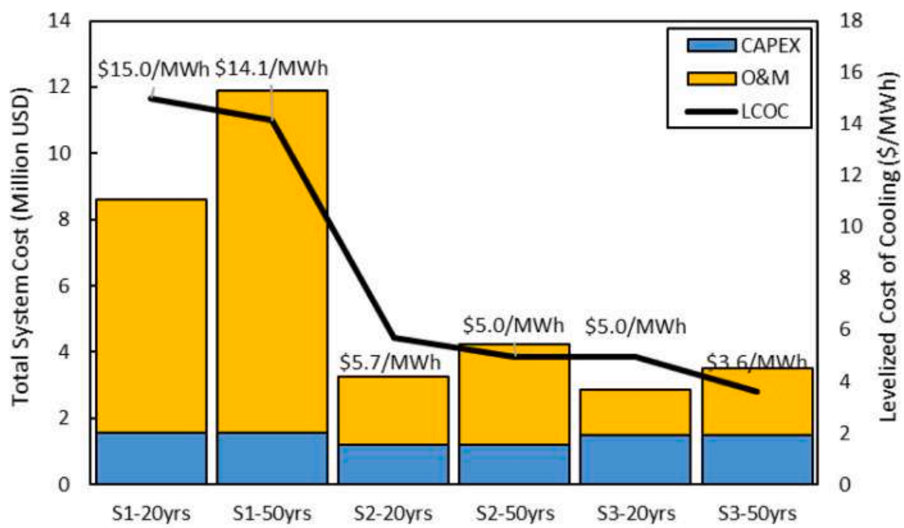

(c)

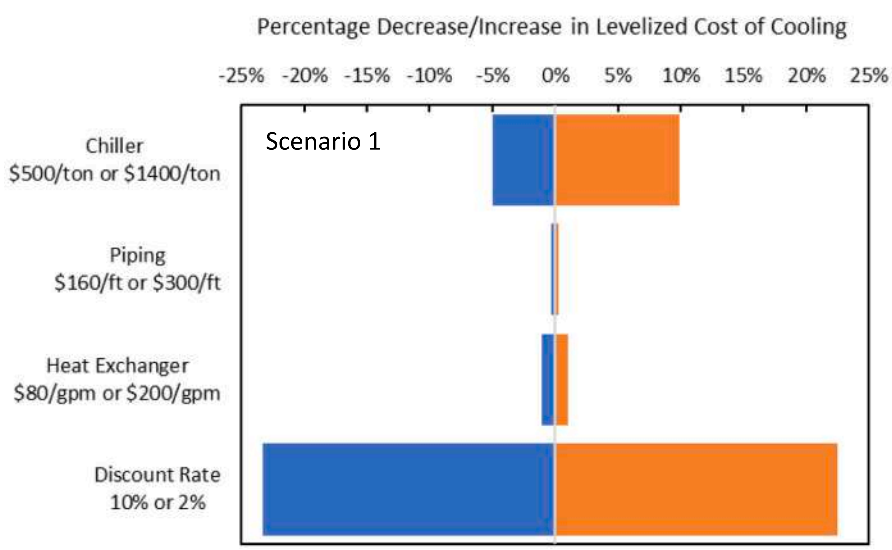

(d)

Fig. 9. (*continued*).

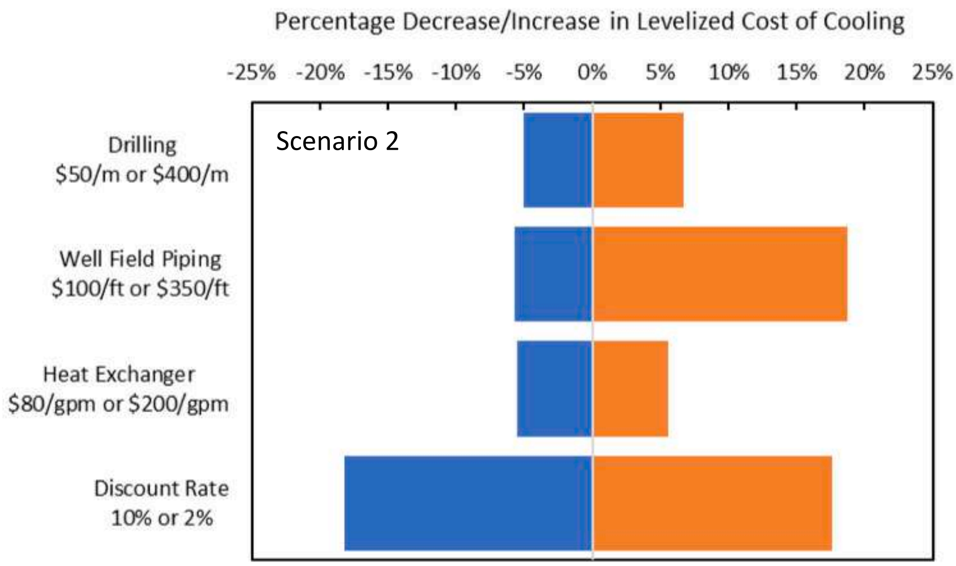

(e)

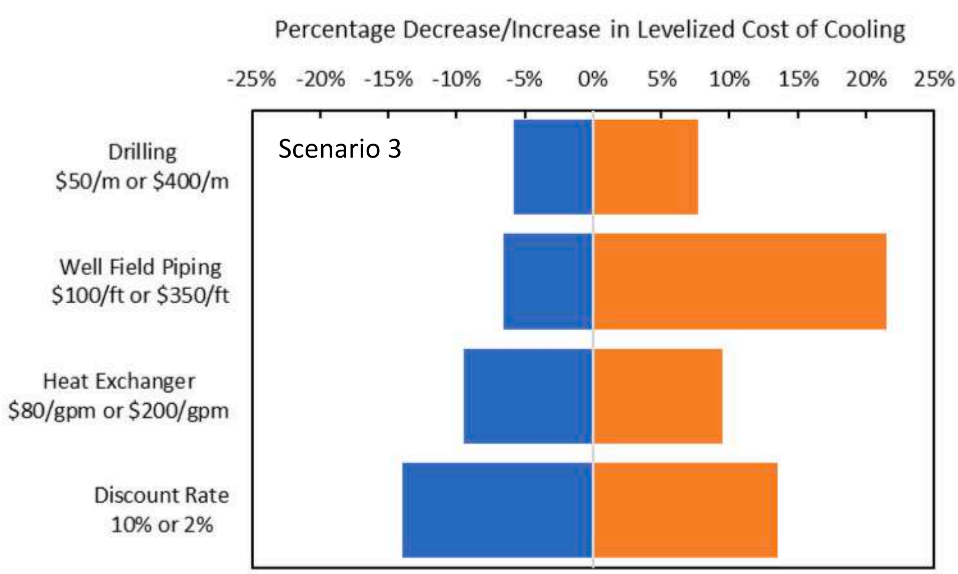

(f)

Fig. 9. (*continued*).

MWh in Scenario 3, depending on the assumptions. Similar to the sensitivity of the LCOC to electricity rates, the sensitivity analysis with the four key drivers demonstrated that the discount rate significantly affected the LCOC. This result suggests that the LCOC can be reduced by optimizing long-term operational strategies, such as reduced long-term operational risks and costs (optimized with grid cost projections), rather than by reducing the CAPEX of the key components.

5. Conclusion

In this study, we evaluated the techno-economic performance of data center cooling systems incorporating RTES. We optimized operational conditions of the RTES, chillers (base case), and dry coolers in terms of the regional subsurface and ambient conditions to supply the 5 MW data center cooling load. We highlight three primary conclusions from this study. First, the RTES has capabilities to reliably supply the data center cooling load for 20 years by storing cold water into the RTES during winter. The COP of overall systems (that is, a ratio of useful cooling power delivered to electricity consumption) is 11.8, 39.7, and 54.1 in Scenarios 1–3, respectively. During peak summer in Mode 1, the COPs of chillers in Scenario 1 and the RTES in the two RTES scenarios are 2.4 and 16.5, respectively, highlighting operational benefits of the RTES. Second, the RTES system significantly saved annual electricity consumption and operational costs as well as capital costs. The heat recovery system further reduces the peak and annual electricity consumption and operational cost. Lastly, the LCOC of $15/MWh in Scenario 1 significantly decreases to $5.7/MWh with the RTES in Scenario 2 and $5/MWh with the RTES and heat recovery system in Scenario 3. The two RTES scenarios also show lower LCOC than Scenario 1 under different assumptions for cost estimations from optimistic to conservative, even with the RTES systems doubly sized to address uncertainties in the subsurface conditions. The LCOC of the RTES-based cooling systems decreases with an increase in the system lifetime. In addition to the reliability and economic benefits of the RTES system, the RTES system annually avoids a considerable amount of CO_2 emissions as compared to the chiller-based cooling system in Scenario 1: Emissions of 1335 tCO_2e and 1488 tCO_2e are avoided with Scenario 2 and Scenario 3, respectively. These results demonstrate the RTES could be utilized as an energy-efficient and cost-effective cooling system for data centers.

For future studies, we suggest extending the RTES system design to combine chillers and dry coolers for supplying cold water at a lower temperature than 21 °C. The economic benefits of computational performance enhanced by cooling ICT equipment to lower temperatures is another area worthy of future study. Chiller operations could be optimized to more economically supply colder water during off-peak hours rather than during the peak summer designed in Scenario 1. Similarly, chillers and dry coolers in the non-RTES base scenario could be further optimized through the off-peak chiller operations while a traditional cold energy storage system meets the data center cooling load during peak summer. Additionally, assessing the value of these cooling systems—optimized for a lower supply temperature, accounting for both ambient conditions and electricity rates—in the electrical grid is crucial to understand the regional impact, especially in a grid heavily reliant on fossil fuel power stations. Finally, we suggest analyzing the resilience of the RTES-based cooling system under extreme heat where free-cooling alternatives may not be available, and the cost of compressor-based cooling systems increases.

CRediT authorship contribution statement

Hyunjun Oh: Writing – original draft, Visualization, Validation, Resources, Methodology, Investigation, Formal analysis, Data curation, Conceptualization. **Wencheng Jin:** Writing – original draft, Methodology, Investigation, Formal analysis. **Peng Peng:** Writing – original draft, Methodology, Investigation, Formal analysis, Conceptualization. **Jeffrey A. Winick:** Writing – review & editing, Validation, Supervision, Conceptualization. **David Sickinger:** Writing – review & editing, Resources, Methodology, Investigation, Formal analysis, Conceptualization. **Dale Sartor:** Writing – review & editing, Validation, Resources, Methodology, Investigation, Conceptualization. **Yingqi Zhang:** Writing – review & editing, Validation, Supervision, Resources, Project administration, Methodology, Investigation, Funding acquisition, Conceptualization. **Koenraad Beckers:** Writing – review & editing, Validation, Resources, Methodology, Funding acquisition, Conceptualization. **Kevin Kitz:** Writing – review & editing, Validation, Supervision, Methodology, Data curation, Conceptualization. **Diana Acero-Allard:** Writing – review & editing, Supervision, Resources, Project administration, Data curation. **Trevor A. Atkinson:** Writing – review & editing, Validation, Supervision, Resources, Project administration, Funding acquisition, Conceptualization. **Patrick Dobson:** Writing – review & editing, Validation, Supervision, Resources, Methodology, Funding acquisition, Conceptualization.

Declaration of competing interest

The authors declare the following financial interests/personal relationships which may be considered as potential competing interests: This work was supported by the U.S. Department of Energy (DOE), Office of Energy Efficiency and Renewable Energy, Geothermal Technologies Office (GTO), under Contract No. DE-AC36-08GO28308 with the National Renewable Energy Laboratory (NREL), Contract Number DE-AC07-05ID14517 with Idaho National Laboratory (INL), and Contract Number DE-AC02-05CH11231 with Lawrence Berkeley National Laboratory (LBNL). The views expressed in the article do not necessarily represent the views of the DOE or the U.S. Government. The U.S. Government retains and the publisher, by accepting the article for publication, acknowledges that the U.S. Government retains a nonexclusive, paid-up, irrevocable, worldwide license to publish or reproduce the published form of this work, or allow others to do so, for U.S. Government purposes. All authors approve the manuscript for submission and declare that we have no competing interests. The authors also confirm that AI/AI-assisted technologies were not used in the manuscript.

Acknowledgement

This work was supported by the U.S. Department of Energy (DOE), Office of Energy Efficiency and Renewable Energy, Geothermal Technologies Office (GTO), under Contract No. DE-AC36-08GO28308 with the National Renewable Energy Laboratory (NREL), Contract Number DE-AC07-05ID14517 with Idaho National Laboratory (INL), and Contract Number DE-AC02-05CH11231 with Lawrence Berkeley National Laboratory (LBNL). The views expressed in the article do not necessarily represent the views of the DOE or the U.S. Government. The U.S. Government retains and the publisher, by accepting the article for publication, acknowledges that the U.S. Government retains a nonexclusive, paid-up, irrevocable, worldwide license to publish or reproduce the published form of this work, or allow others to do so, for U.S. Government purposes. We thank Industrial Advisory Group members for their feedback. We also thank Sean Porse, Andy Adams, and Lindsey Baker from the DOE GTO and Amy Brice, Mark Ruth, Amanda Kolker, Craig Turchi, and Matthew Thornton at NREL for their helpful input and reviews.

Data availability

Source data and methodologies are available in the article. The Multiphysics Object-Oriented Simulation Environment (MOOSE) finite-element model codes are available from. https://github.com/idaholab/moose/tree/2022-06-10-release.

References

[1] Andrae ASG, Edler T. On global electricity usage of communication technology: trends to 2030. Challenges 2015;6(1):117–57. https://doi.org/10.3390/challe6010117.

[2] Liu Y, Wei X, Xiao J, Liu Z, Xu Y, Tian Y. Energy consumption and emission mitigation prediction based on data center traffic and PUE for global data centers. Global Energy Interconnection 2020;3(3):272–82. https://doi.org/10.1016/j.gloei.2020.07.008.

[3] Lei N, Masanet ER. Global data center energy demand and strategies to conserve energy. In: Chapter 2 in Data Center Handbook: Plan, Design, Build, and Operations of a Smart Data Center. New Jersey, U.S: Second Edition, Wiley; 2021. https://doi.org/10.1002/9781119597537.ch2.

[4] de Vries A. The growing energy footprint of artificial intelligence. Joule 2023;7 (10):2191–4. https://doi.org/10.1016/j.joule.2023.09.004.

[5] Shehabi A, Smith SJ, Hubbard A, Newkirk A, Lei N, Siddik MAB, et al. 2024 United States data center energy usage report. Technical Report,. Lawrence Berkeley National Laboratory, Berkeley, California: LBNL-2001637; 2024.

[6] Masanet E, Shehabi A, Lei N, Smith S, Koomey J. Recalibrating global data center energy-use estimates. Science 2020;367:984–6.

[7] Electricity 2024 – Analysis and forecast to 2026. In: International energy agency (IEA). International Energy Agency; 2024.

[8] Greenberg S, Mills E, Tschudi W. Best practices for data centers: Lessons learned from benchmarking 22 data centers. 2006 [In ACEEE Summer Study on Energy Efficiency in Buildings].

[9] Brown R, Masanet E, Nordman B, Tschudi W, Shehabi A, Stanley J, et al. Report to congress on server and data center energy efficiency. Public Law 109-431,. Lawrence Berkeley National Laboratory; 2008.

[10] Oh H, Beckers K, McCabe K. Geospatial characterization of low-temperature heating and cooling demand in residential, commercial, manufacturing, agricultural, and data center sectors for potential geothermal applications in the United States. Renew Sust Energ Rev 2024;206:114875.

[11] Electric Power Research Institute (EPRI). Powering intelligence: Analyzing artificial intelligence and data center energy consumption. In: 2024 white paper, Electric Power Research Institute; 2024.

[12] Shehabi A, et al. United States data center energy usage report. Lawrence Berkeley National Laboratory; 2016.

[13] Zhang Q, Meng Z, Hong X, Zhan Y, Liu J, Dong J, et al. A survey on data center cooling systems: technology, power consumption modeling and control strategy optimization. J Syst Archit 2021;119:102253. https://doi.org/10.1016/j.sysarc.2021.102253.

[14] Carter T, Liu Z, Sickinger D, Regimbal K, Martinez D. Thermosyphon Cooler Hybrid System for Water Savings in an Energy-Efficient HPC Data Center: Modeling and Installation. In: Presented at the 2017 ASHRAE winter conference, Las Vegas, Nevada; 2017.

[15] Sickinger D, Van Geet OD, Belmont SA, Carter T, Martinez D. Thermosyphon cooler hybrid system for water Savings in an Energy-Efficient HPC data center: Results from 24 months and the impact on water usage effectiveness. Technical Report, NREL/TP-2C00-72196,. Golden, Colorado: National Renewable Energy Laboratory; 2018. https://doi.org/10.2172/1471661.

[16] Lei N, Masanet E. Climate- and technology-specific PUE and WUE estimations for U.S. data centers using a hybrid statistical and thermodynamics-based approach. Resources, Conversion Recycling 2022;182:106323. https://doi.org/10.1016/j.resconrec.2022.106323.

[17] Zhang Y, Zhao Y, Dai S, Nie B, Ma H, Li J, et al. Cooling technologies for data centres and telecommunication base stations – a comprehensive review. J Clean Prod 2022;334:130280.

[18] Ebrahimi K, Jones G, Fleischer A. A review of data center cooling technology, operating conditions and the corresponding low-grade waste heat recovery opportunities. Renew Sust Energ Rev 2014;31:622–38.

[19] Yu J, Jiang Y, Yan Y. A simulation study on heat recovery of data center: a case study in Harbin. China Renew Energy 2019;130:154–73.

[20] Fleuchaus P, Godschalk B, Stober I, Blum P. Worldwide application of aquifer thermal energy storage – a review. Renew Sust Energ Rev 2018;94:861–76.

[21] Burns E, Bershaw J, Williams C, Wells R, Uddenberg M, Scanlon D, et al. Using saline or brackish aquifers as reservoirs for thermal energy storage, with example calculations for direct-use heating in the Portland Basin, Oregon, USA. Geothermics 2020;88:101877.

[22] Atkinson T, Ginosar D, Adhikari B, Toman J, Podgorney J. Reservoir thermal energy storage benchmarking. Idaho National Laboratory; 2023.

[23] Pepin J, Burns E, Dickinson J, Duncan L, Kuniansky E, Reeves H. National-scale reservoir thermal energy storage pre-assessment for the United States. In: Proc., 46th workshop on geothermal reservoir engineering. Stanford University; 2021.

[24] Jin W, Atkinson T, Doughty C, Neupane G, Spycher N, McLing T, et al. Machine-learning-assisted high-temperature reservoir thermal energy storage optimization. Renew Energy 2022;197:384–97.

[25] Dobson P, et al. Hybrid uses of high-temperature reservoir thermal energy storage: lessons learned from previous projects. In: In the SPE energy transition symposium, SPE-215750-MS; 2023.

[26] Zhang Y, et al. Addressing data center cooling needs through the use of subsurface thermal energy storage systems. In: In the SPE energy transition symposium, (SPE-215746-MS); 2023.

[27] David M, Schmidt. Impact of ASHRAE environmental classes on data centers. In: *Fourteenth Intersociety Conference on Thermal and Thermomechanical Phenomena in Electronic Systems (ITherm)*, Orlando, Florida; 2014. p. 1092–9. https://doi.org/10.1109/ITHERM.2014.6892403.

[28] Azarifar M, Arik M, Chang J. Liquid cooling of data centers: a necessity facing challenges. Appl Therm Eng 2024;247:123112. https://doi.org/10.1016/j.applthermaleng.2024.123112.

[29] ASHRAE–American Society of Heating. Refrigerating, and Air-Conditioning Engineers. In: 2021 Equipment Thermal Guidelines for Data Processing Environments. ASHRAE TC 9.9 Reference Card. *5th ed.* 2021. ASHRAE.

[30] Dechesne M, Raynolds RG, Barkmann PE, Johnson KR. Notes on the Denver Basin geologic maps: Bedrock geology, structure, and isopach maps of the upper cretaceous through Paleocene strata between Greeley and Colorado Springs. Colorado Geological Survey: Colorado; 2011.

[31] Anderson DS, Haseman PB. Golden rocks: The geology and mining history of Golden. Golden, Colorado: Colorado. Books-Russell L. & Lyn Wood Mining History Archive; 2022.

[32] Wilkins A, Green CP, Ennis-King J. An open-source multiphysics simulation code for coupled problems in porous media. Comput Geosci 2021;154:104820.

[33] Permann CJ, Gaston DR, Andrš D, Carlsen RW, Kong F, Lindsay AD, et al. MOOSE: enabling massively parallel multiphysics simulation. SoftwareX 2020;11:100430.

[34] Jin W, Podgorney R, McLing T. THM coupled numerical analysis on the geothermal energy storage and extraction in porous fractured reservoir. In: ARMA-2020-1338, Presented at the 54th U.S. Rock Mechanics/Geomechanics Symposium (physical event cancelled); 2020.

[35] Musgrove M, Beck JA, Paschke SS, Bauch NJ, Mashburn SL. Quality of groundwater in the Denver Basin aquifer system, Colorado, 2003–5. Scientific investigations report 2014–5051. Colorado: U.S. Department of the Interior. U.S. Geological Survey. Denver; 2014.

[36] Raynolds RG, Johnson KR, Arnold LR, Farnham TM, Fleming RF, Hicks JF, et al. The Kiowa core, a continuous drill core through the Denver Basin bedrock aquifers at Kiowa, Elbert County, Colorado (no. 2001–185). Geological Survey: U.S; 2001.

[37] Ochsner A, T.. Patterns and mechanisms of heat transport in the northern Denver Basin Nebraska, South Dakota and Wyoming. Master's thesis, University of North Dakota; 2014.

[38] Rice A, McCray J, Singha K. Numerical investigation of wellbore methane leakage from a dual-porosity reservoir and subsequent transport in groundwater. Water Resour Res 2021;57. https://doi.org/10.1029/2019WR026991.

[39] Dechesne M, Raynolds RG, Barkmann PE, Johnson KR. Notes on the Denver Basin geologic maps: Bedrock geology. Structure and Isopach maps of the upper cretaceous through Paleocene strata between Greeley and Colorado Springs, Colorado. Golden, Colorado: Colorado Geological Survey; 2011.

[40] Peng P, Anastasopoulou A, Brooks K, Furukawa H, Bowden M, Long J, et al. Cost and potential of metal–organic frameworks for hydrogen back-up power supply. Nat Energy 2022;7:448–58.

[41] Oh H, Akar S, Beckers K, Bonnema E, Vivas C, Salehi S. Techno-economic feasibility of geothermal energy production using inactive oil and gas wells for district heating and cooling systems in Tuttle. Oklahoma Energy Conv Manag 2024;308:118390.

[42] EIA. U.S. Energy Information Administration. In: Colorado Electricity Profile 2023. Table 1. 2023 Summary Statistics (Colorado); 2024. Available from: https://www.eia.gov/electricity/state/colorado/.

[43] Lowry TS, Finger JT, Carrigan CR, Foris A, Kennedy MB, Corbett TF, et al. GeoVision analysis supporting task force report: Reservoir maintenance and development. Sandia National Laboratories; 2017.

[44] Mines GL. GETEM User Manual. Idaho National Laboratory; 2016.

[45] Augustine CR. Hydrothermal spallation drilling and advanced energy conversion Technologies for Engineered Geothermal Systems. PhD Dissertation,. Cambridge, MA: Massachusetts Institute of Technology; 2009.

[46] Moser M, Trieb F, Fichter T, Kern J, Maier H, Schicktanz P. Techno-economic analysis of enhanced dry cooling for CSP. Energy Procedia 2014;49:1177–86.

[47] EIA. U.S. Energy Information Administration. In: *U.S. Energy Facts Explained*. U.S; 2024. Available from: (2024), https://www.eia.gov/energyexplained/us-energy-facts/.

[48] EPA. U.S. Environmental Protection Agency. In: Global Greenhouse Gas Overview; 2024. Available from: https://www.epa.gov/ghgemissions/global-greenhouse-gas-overview (2024).

[49] Kartal MT, Ulussever T, Pata UK, Depren SK. Time and frequency analysis of daily-based nexus between global CO2 emissions and electricity generation nexus by novel WLMC approach. Sci Rep 2024;14:3698.

[50] Shen L, Jacob DJ, Gautam R, Omara M, Scarpelli TR, Lorente A, et al. National quantifications of methane emissions from fuel exploitation using high resolution inversions of satellite observations. Nature Comm 2023;14:4948.

[51] Sherwin ED, et al. US oil and gas system emissions from nearly one million aerial site measurements. Nature 2024;627:328–34.

[52] EPA. U.S. Environmental Protection Agency. In: 1.4 Natural Gas Combustion; 1998. Available from: https://www.epa.gov/sites/default/files/2020-09/documents/1.4_natural_gas_combustion.pdf.

[53] Cho K, Chang H, Jung Y, Yoon Y. Economic analysis of data center cooling strategies. Sustain Cities Soc 2017;31:234–43. https://doi.org/10.1016/j.scs.2017.03.008.

[54] Liu C, Hao N, Zhang T, Wang D, Li Z, Bian W. Optimization of data-center immersion cooling using liquid air energy storage. J Energy Storge 2024;90:111806. https://doi.org/10.1016/j.est.2024.111806.

[55] Alipour M, Deymi-Dashtebayaz M, Asadi M. Investigation of energy, exergy, and economy of co-generation system of solar electricity and cooling using linear parabolic collector for a data center. Energy 2023;279:128076. https://doi.org/10.1016/j.energy.2023.128076.

[56] Beckers KF, Kolker A, Pauling H, McTigue JD, Kesseli D. Evaluating the feasibility of geothermal deep direct use in the United States. Energy Convers Manag 2021;243:114335.